Connecting lignin gasification with syngas fermentation

E.T. Liakakou[1*†], A. Infantes[2†], A. Neumann[2], B.J. Vreugdenhil[1]

[1] TNO Energy Transition, Biomass & Energy Efficiency Unit, Westerduinweg 3, Petten, 1755 LE, Netherlands

[2]KIT, Institute of Process Engineering in Life Science 2: Technical Biology, Karlsruhe Institute of Technology, Fritz-Haber-Weg 4, 76131 Karlsruhe, Germany

† Liakakou and Infantes share first authorship

***Corresponding Author**

Eleni T. Liakakou

e-mail: eleni.liakakou@tno.nl

phone: +31 6 5000 9668

Abstract

The development of lignin derived energy products is one way to increase the value of biorefinery residues, which is the scope of the EU project AMBITION. Gasification of (lignin-rich) biorefinery residues, followed by product gas cleaning and anaerobic fermentation, offers a potential to produce higher added-value products such as biofuels and chemicals.

MILENA indirect gasification allows complete fuel conversion and produces a high value gas composed of CO, H_2 and CO_2, as well as compounds such as CH_4, C_2-C_4 gases, benzene, toluene and xylene (BTX). The separation of the most valuable components of the product gas is a good way to maximize the value from the feedstock via co-production schemes. The product gas, after appropriate cleaning to remove impurities that can reduce the fermentability of syngas, can be applied in the gas fermentation process.

Some anaerobic microorganisms, known as acetogens, can be used as a biocatalyst for the conversion of syngas into short-chain organic acids and alcohols, like acetate, ethanol, butanol, butan-2,3-diol and butyric acid. The ability of these microorganisms to withstand some of the impurities contained in the syngas and their flexibility to use different mixtures of CO and/or CO_2 and H_2 makes these bacteria an attractive alternative to the chemical catalytic processes.

Despite these advantages, the integration of gasification with syngas fermentation is still in an early stage of development, where many questions exist concerning the syngas quality needed in the fermentation process. The challenge is to define the optimum gasification conditions for this type of feedstock that will provide a H_2:CO:CO_2 ratio at values suitable for syngas fermentation, as well as to identify and remove the compounds that can inhibit the performance of the microorganisms. In this work a first attempt to combine the two processes is presented.

A lignin rich feedstock was gasified with steam at 780°C using MILENA indirect gasifier, at TNO. The product gas after removal of the main impurities, consisted of CO, H_2, CO_2, N_2, CH_4 and traces of

other gaseous hydrocarbons, benzene and H_2S. The influence of the obtained syngas quality and composition was evaluated in the fermentation process, at KIT. For comparison, product gas from beech wood gasification after cleaning was also evaluated in the fermentation process under the same conditions.

The process involved growing cells in a batch system under continuous flow of biomass-derived gas. The strain used in this work is *Clostridium ljungdahlii*. The fermentation of both beech wood and lignin-derived syngas was successful, since no inhibition was observed. The carbon fixation onto products achieved for both cases was approximately 55%, while a slightly higher ethanol production was observed with the lignin-derived syngas. The total productivity (including both acetate and ethanol) at the end-point was 0.18 g/L/h for both fermentations.

Keywords

Lignin gasification, indirect gasification, biorefinery, syngas fermentation

1. Introduction

The development of lignin derived energy products is one way to increase the value of biorefinery residues, which is the scope of the EU project AMBITION [1]. Second generation biorefineries for the production of bioethanol use pre-treatment technologies where lignin ends up in a residue together with unconverted fibers, feedstock minerals, and process chemicals. This type of residue is usually exploited in a rather low-added-value application, such as combined heat and power generation. The syngas obtained from gasification of lignin-rich biorefinery residues offers the potential to produce higher-added-value products, such as liquid fuels and chemicals [2, 3, 4, 5].

In a previous study [6], different gasification technologies were compared for the valorization of lignin-rich residues, obtained from the production of second generation bioethanol. The indirect or allothermal gasification allows high feedstock conversion and also better control and process optimization. The combustion products (flue gas) and gasification products (product gas or synthesis

gas) are not mixed. This means that the product gas is not diluted with N_2 coming from the air used for combustion, and thus, is suitable for synthesis applications after proper cleaning and upgrading without the need for an expensive air separation unit. Furthermore, indirect gasification produces a high value gas which contains compounds such as CH_4, C_2-C_4 gases (including ethylene and acetylene), benzene, toluene and xylene (BTX), and tar. The separation of the most valuable components of the product gas is a good way to maximize the value from the feedstock via co-production schemes [7].

The product gas, after appropriate cleaning to remove impurities that can reduce the fermentability of syngas, can be used in a biological process to produce biofuels. Syngas fermentation is a "hybrid thermochemical/biochemical process" because of the nature of the joint process. Acetogenic bacteria can be used as biocatalysts for the microbial conversion of syngas into short-chain organic acids and alcohols, such as ethanol and acetate [8, 9, 10]. The ability of these microorganisms to withstand some of the impurities contained in the syngas and their flexibility to use different mixtures of CO and/or CO_2 and H_2 makes them an attractive alternative to the chemical catalytic processes. Moreover, the process conditions used are milder, resulting in reduced operating costs [10, 11]. However, the integration of gasification with syngas fermentation is still in an early stage of development, where many questions exist concerning the syngas quality needed in the fermentation process.

For the integration of biomass gasification and syngas fermentation, it is of utmost importance to understand how the different feedstocks impact the final syngas composition, and which impurities and inhibitory compounds are present in the final syngas, since this two factors have a strong influence in the fermentation outcome [12, 13]. With this information, the syngas production and cleaning strategy can be optimized to improve the fermentation outcome.

According to the literature [14, 15, 16, 17], the main requirement for syngas for fermentation is low contents of contaminants like tar, acetylene, ethylene and benzene, as they inhibit enzymes

responsible for the initial harvesting of carbon and energy from syngas in acetogenic organisms. Most of the organisms grow better by using CO as the only energy and carbon source or with CO as the carbon source and CO/H_2 as the energy source [18]. As a result, the H_2 to CO ratio can be low, i.e. additional reforming steps and water-gas shift reaction after gasification is not needed. Most acetogens are also able to grow and produce ethanol from CO_2 and H_2, providing direct CO_2 sequestration into products [19]. However, many of these requirements, such as the tolerance to sulphur, will depend on the particular type of organism used [20].

Syngas fermentation has been chosen as an attractive conversion route by several companies for pilot-, demo- and near commercial-scale cellulosic ethanol production [8]. However, two of the three companies that operate scaled up gas fermentation facilities suspended their operation by 2016 [21]. Coskata was addressing ethanol production in a demo- unit, first using syngas from biomass gasification and later from methane reforming, but went out of business in 2015 [22]. INEOS New Planet BioEnergy, developed a syngas-to ethanol process, but stopped the operations by 2016 due to the high levels of hydrogen cyanide in syngas [23]. LanzaTech is deploying two commercial ethanol-producing facilities using off-gases and is also moving towards the biomass sector with two commercial-scale projects under development, using syngas produced from agricultural waste and municipal solid waste [24, 25].

Despite the recent developments, challenges associated with the scale-up and operation of this novel process, such as low mass transfer efficiency and the presence of inhibitory compounds in syngas still remain. In this work we report a first approach to combine the indirect gasification of lignin-rich residues with syngas fermentation. The important focus point is the gas quality, since the requirements for syngas fermentation are different compared to a chemical catalytic processes. The product gas from the lignin-rich feedstock gasification is utilized in the fermentation process using *C. ljungdahlii* for the production of acetate and ethanol, after appropriate cleaning and conditioning to remove impurities that can reduce the fermentability of the gas (such as tars, BTX, unsaturated

hydrocarbons, HCN, HCl, COS and other organic S-compounds). Product gas from beech wood gasification is also utilized in the fermentation process under the same conditions, in order to compare the two feedstocks.

2. Experimental

Feedstock properties

The lignin-rich feedstock, which was received from a biorefinery, is originating from wheat straw and was filter pressed, therefore consisted of big dense particles. The pretreatment of this feedstock (from now on referring as lignin) was described in detail elsewhere [6]. Beech wood was received in chips and no pretreatment was required before feeding in the gasifier. The feedstocks as used in the indirect gasification tests are shown in Figure 1.

Table 1 summarises the thermochemical properties of the feedstocks. As can be seen, the amount of volatile matter is lower for lignin compared to beech wood. What stands out is the high ash content of lignin (14 wt.%) that mainly consists of silica (5.4 wt.% of the feedstock), with minor amounts of calcium (0.5 wt.%) and potassium (0.3 wt.%). This could lead to agglomeration and corrosion issues at high temperatures (above 900°C), due to alkali-silicate melt phase formation on the bed material [26, 27]. For this reason it was decided to perform the lignin gasification test at lower temperature than beech wood (<800°C). Furthermore, the sulphur and nitrogen content of lignin is relatively high compared to wood, which can lead to high S- and N- compounds in the product gas (such as H_2S, COS, NH_3, etc.). Depending on the resistance of the micro-organisms to these compounds, a suitable gas conditioning method needs to be applied for their removal.

Table 1. Thermochemical properties of lignin and beech wood feedstocks

	Lignin	**Beech wood**
Moisture content 105°C (wt.%, as received)	36	9
Ultimate analysis (wt.%, dry basis)		
C	47.2	48.8
H	5.6	6.0
O	33.0	44.5
N	1.3	0.14
S	0.18	0.02
Cl	0.020	0.005
Proximate analysis (wt.%, dry basis)		
Ash 550°C	14.0	1.0
Volatile matter	64.6	83.0
Lower heating value (MJ/kg)	18.4	17.8
ICP analysis (mg/kg, dry basis)		
Al	380	48
As	< 3	0.8
B	1	3.4
Ba	96	11
Ca	4750	2707
Cd	0	0.1
Co	1	24
Cr	8	0.5

Cu	8	1.7
Fe	290	27
K	3250	1173
Li	< 0.6	n/m
Mg	385	365
Mn	53	51
Mo	< 2	0.8
Na	906	13
Ni	3	0.9
P	930	88
Pb	< 1	5.2
S	1750	200
Sb	< 7	0.8
Se	< 3	1.4
Si	54000	168
Sn	< 2	0.6
Sr	10	4.4
Ti	13	1.5
V	1	0.1
W	14	n/a
Zn	15	2.8

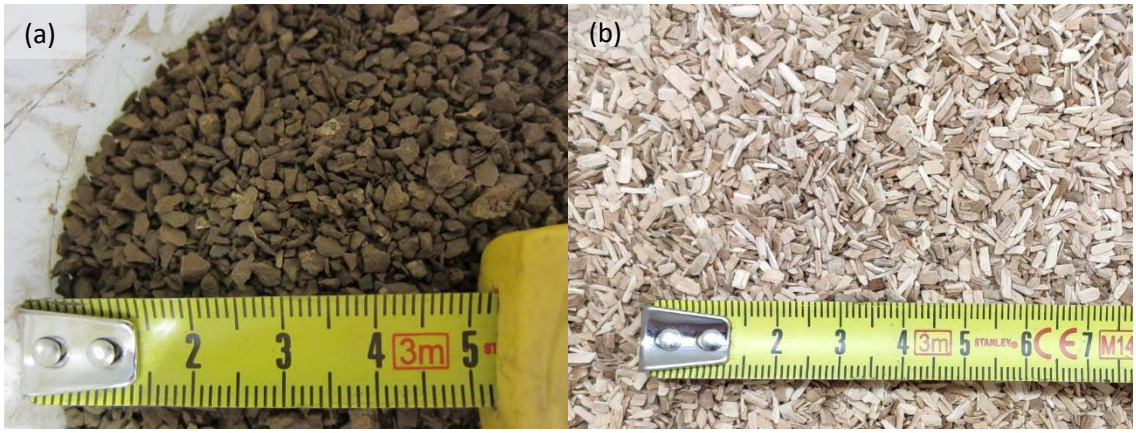

Figure 1. Lignin (a) and beech wood (b) as used in the gasification tests.

Description of the experimental set-ups and product analysis

MILENA Indirect gasification

The MILENA gasifier was developed for the gasification of biomass and the process is based on indirect or allothermal gasification [28]. In one reactor the fuel is gasified or pyrolyzed using hot bed material. Because of the relatively low temperature (typically 850°C) of the pyrolysis process the conversion of the fuel is limited. The remaining char is combusted in a separate reactor. The heat from the combustion is used to heat the circulating bed material. In the typical wooden biomass configuration the gasification takes place in the riser reactor where the residence time of the fuel is relatively short, but sufficient for the reactive biomass.

After the previous test in riser gasification mode with the same lignin [6], the results showed that the fuel conversion was insufficient, so the MILENA configuration was converted to operate inversely. A schematic layout and a picture of the of the so-called i-MILENA concept is given in Figure 2. Biomass is added to the bubbling fluidized bed zone (BFB) via a feeding screw. The BFB acts as steam gasification reactor, thus allowing longer residence times (in the order of 10 – 20 minutes) of the fuel particles compared to the MILENA concept in order to cope with less reactive (low volatile, high ash) feedstock. Furthermore, the process conditions in the steam blown bubbling fluidized bed gasifier are optimum for primary tar reduction, because an excess steam is available for tar

reforming and the contact between the (catalytic) bed material is better than the riser. The heat required for the endothermic steam gasification reactions is created by combustion of the remaining coke in the riser zone using air. Additional heat is provided to the BFB reactor by tracing, due to the restricted size of the riser combustor. Hot bed material ejected from the top of the riser is separated from flue gas in the settling chamber and recirculated through the downcomer to the BFB gasification zone. Producer gas leaves the gasifier on the side and exits the system via a cyclone.

Fresh Austrian olivine, a mineral based on an iron-magnesium orthosilicate structure ($FeMgSiO_4$), was employed as the bed material. CO_2 was used to flush the fuel feeding screw and to carry the steam in the riser combustor reactor. The detailed operating conditions are shown in Table 2. The gasification temperature was approximately 760°C for lignin and 860°C for beech wood and steam fluidization was conducted at 2.2 kg/h and 1.0 kg/h, respectively. Higher steam flow was used for lignin gasification to reach the minimum fluidization velocity in the BFB. Additional nitrogen was also used periodically (as indicated in Figure 13) in this lab-scale test, to compensate for reduced gas flow in the BFB, due to difficulties feeding sufficient feedstock. The gasification system was operated at atmospheric pressure. Tracer gases, such as Ne and Ar, were added downstream the gasifier for flow determination.

Figure 2. Picture and schematic layout of the 25 kW i-MILENA gasifier as used for lignin and beech wood gasification.

Table 2. Gasification conditions used in i-MILENA indirect gasifier.

Gasification conditions	**Lignin**	**Beech wood**
T in BFB gasifier (°C)	760	860
Fuel, dry (kg/h)	3.4	3.6
Fuel moisture content (wt.%)	3.3	9.0
Steam (kg/h)	2.2	1.0
Carrier gas CO_2 (NL/min)	2.3	2.2
Tracer gas Ne upstream OLGA (NL/min)	0.01	0.01
Tracer gas Ar downstrean MILENA (NL/min)	1	1
Combustion air in riser (NL/min)	100	100

Values are at Normal conditions at temperature of 0 °C (273.15 K) and absolute pressure of 1 atm (1.01325×105 Pa).

Product gas cleaning

The layout of the gasification and gas cleaning process is shown in Figure 3, indicating the product gas sampling positions. A slipstream of dry produced gas from the MILENA gasifier was directed at approximately 1000 NL/h to the system downstream and the rest was sent to the afterburner. The OLGA tar removal unit, a staged oil-based scrubbing system, almost completely separated the gas from tar compounds heavier than BTX [7].

Neon gas was injected at 0.01 NL/min as tracer gas upstream OLGA to be able to check molar balances over the downstream system. Since lignin has a high sulphur content, the product gas contained significant amount of H_2S that was captured by an Activated Carbon (AC) bed, containing a commercial AC adsorbent, operating at 80°C. A fixed bed reactor was used, with external trace heating and a series of thermocouples to measure the axial temperature profile over the reactor.

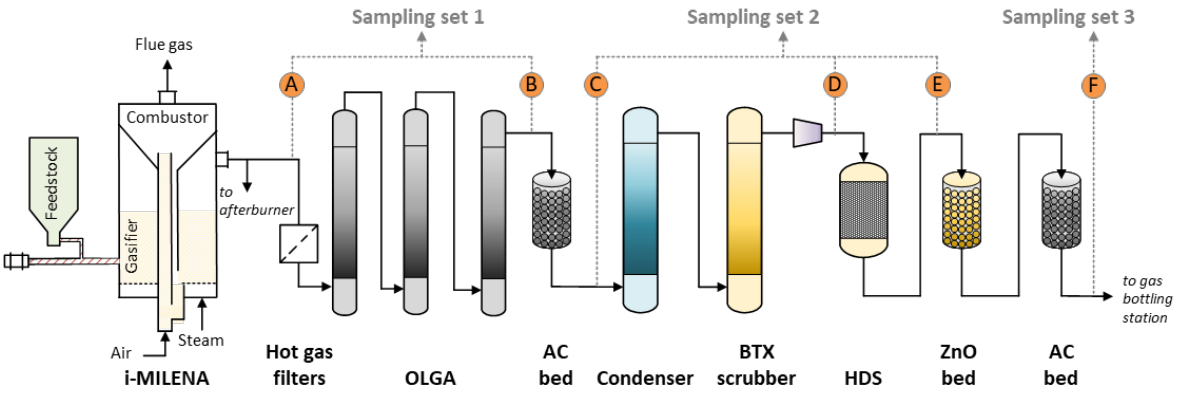

Figure 3 Experiment layout of the gasification and gas cleaning process, as applied during the gas bottling campaigns at TNO. The product gas sampling positions are also indicated.

Subsequently, most of the water in the product gas was removed by a condenser operating at 10 °C to reduce the gas moisture content to around 1%. The condenser (see Figure 3) does not only remove water from product gas. It can have a large effect on water soluble compounds, especially HCl and NH_3 (not measured here). The gas flow varies over time when the flow resistance over the system changes. Flow resistance varies mainly over the hot gas filter upstream OLGA. The BTX

scrubber which was developed by TNO (shown in Figure 3 and Figure 4), is a system for the separation of BTX and traces of additional hydrocarbons using an absorption liquid. It consists of an absorber and stripper column that are filled with structured packing. A dedicated oil absorbs selectively BTX in the absorber at 35°C. The absorption liquid loaded with BTX is subsequently stripped from BTX using steam in the stripper column. The clean and dry product gas was compressed to about 5 bar by a frequency-regulated compressor. This compressor controls the flow through the units downstream MILENA and thereby the slipstream.

A commercial CoMoO catalyst is used in the hydrodesulphurisation (HDS) reactor, in order to convert the organic sulphur compounds (e.g. thiophene) into mainly H_2S and COS, and hydrogenate alkenes and alkynes into alkanes (e.g. C_2H_4 and C_2H_2 into C_2H_6). The HDS unit (shown in Figure 4) consists of a catalytic fixed-bed reactor with three external trace heating zones to compensate for heat loss and thermocouples along the reactor axis. The water gas shift (WGS) reaction can also take place in this reactor. The operating pressure is approximately 5 bar and the trace heating zones are set at 300°C (top), 370°C (middle), and 480°C (bottom). The target flow rate of gas entering the HDS was 11-12 NL/min in order to keep a GHSV (Gas Hourly Space Velocity) of 200-250 h^{-1}.

The produced H_2S (and COS) is removed from the gas downstream in two adsorption beds (shown in Figure 3 and Figure 4). Both fixed bed reactors are provided with external trace heating and a series of thermocouples to measure the axial temperature profile over the length of the reactor. The first fixed bed contains a commercial AC adsorbent and operates at room temperature and 5 bar. The second contains a commercial ZnO adsorbent and is kept at a temperature of 250°C and pressure of 5 bar. Traces of BTX are also captured by the ZnO and AC adsorption beds.

The product gas is cooled to 4°C to remove any traces of water before it is bottled. Since the bottles were received by the supplier with N_2 atmosphere (3-4 bar), in order to minimize its concentration in the bottles, the bottling procedure is: Releasing the N_2 from the bottles (down to 0.5-1.2 bar), fill one time with product gas up to 5 bar, flush the content down to 0.5-0.9 bar and fill again with

product gas up to the maximum system pressure (5 bar). In total, 750L of clean product gas from beech wood and 750L from lignin gasification were bottled and sent to KIT for the fermentation experiments.

Figure 4 Picture of OLGA (left), BTX scrubber (middle), HDS unit and fixed bed reactors for sulphur removal (right).

Product gas analysis

The product gas was sampled for analysis at 6 different positions: A – F (see Figure 3) using three different sampling sets. Sampling set 1 (S1) was used for the raw product gas (position A: downstream MILENA gasifier and position B: downstream OLGA), sampling set 2 (S2) was used for the conditioned gas (position C: downstream the AC bed, position D: downstream the condenser and BTX scrubber, position E: downstream the HDS reactor) and sampling set 3 (S3) was used for the clean gas after the ZnO and the final AC guard bed (position F: before gas bottling station).

At every gas analysis sampling position, a slip stream of the product gas was cooled down to 5 °C in order to remove the condensate (water and tars) from the gas, thus protecting each gas analysis set. Online monitoring of product gas (H_2, CO, CO_2, CH_4) and flue gas (O_2, CO_2, CO, CxHy, N_2O, NO, NO_2) was carried out by the three analysis sets. ABB CALDOS 17 Thermal Conductivity Detector was used

for H_2, ABB URAS 14 Non Dispersive Infra-Red Analyser (NDIR) for CO, CO_2, CH_4, N_2O, SO_2, ABB MAGNOS 16 Para- Magnetic O_2 sensor for O_2, Ratfisch RS55 Flame Ionisation detector was used for the trace hydrocarbons in the flue gas and ABB LIMAS 11 UV detectors for NO and NO_2. Complementary, the product gas composition was measured online, by the three analysis sets, using micro-GC (Varian Micro-GC CP 4900). The product gas was also sampled for offline analysis of the trace hydrocarbons (GC-FID) and sulphur compounds (GC-FPD). Additionally, the SPA method was used for the determination of the content and composition of the tar compounds in the product gas, at positions A and B, following the CEN/TS 15439:2006 procedure.

Syngas fermentation experimental set-up and analytical methods

The microorganism used for the syngas fermentation was *Clostridium ljungdahlii* DSM 13528. The medium and the cultivation conditions used can be found elsewhere [8]. The fermentations were carried in 3 Minifors bench-top stirred tank reactors, shown in Figure 5 (Infors-HT, Switzerland), which have a total volume of 2.5 L. The working liquid volume is 1.5 L. The gas for the fermentation was supplied by means of a microsparger, while the gas flow rate was controlled via a mass flow controller (MFC) red-y smart series, from Vögtlin Instruments (Switzerland). The temperature of the fermenter was kept at 37°C, pH was controlled at 5.9 with 4M KOH and stirring was regulated at 800 rpm. A detailed description of the fermenter set-up can be found elsewhere [8].

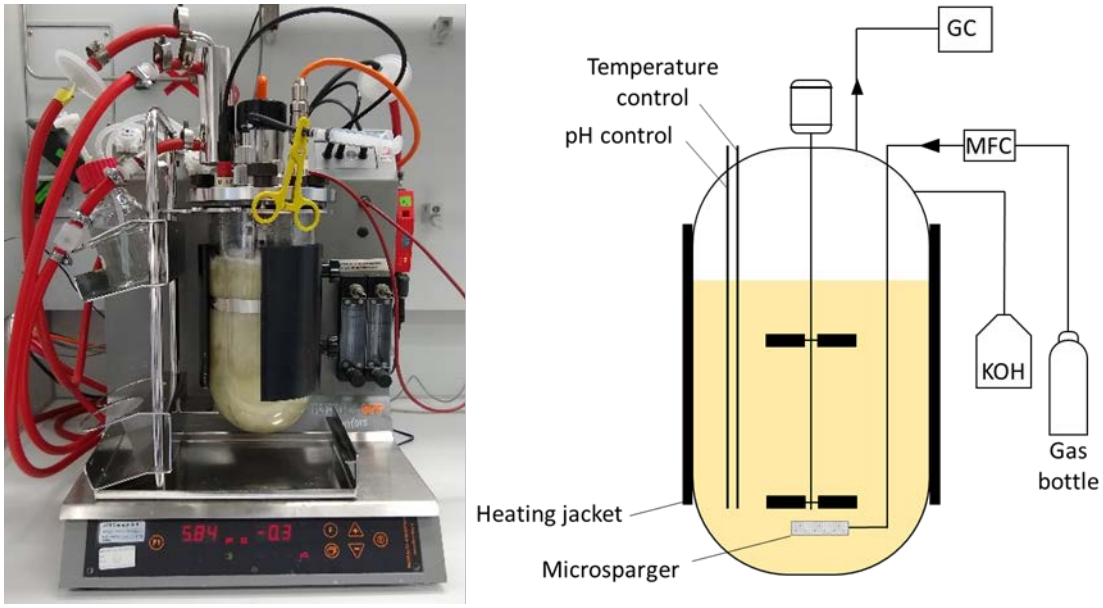

Figure 5. 2 L glass stirred tank reactor used for the syngas fermentation tests

The fermentation experiments were performed using real syngas produced from beech wood and lignin gasification by TNO. Despite the fact that the gas bottling took place after cleaning and conditioning as described in the previous chapter, some unidentified impurities might still be present in the syngas. Anaerobic conditions were ensured after autoclaving by sparging the fermenters with N_2 for 2 h. Following this, the gas supply was changed to syngas with a flow rate of 50 mL/min for at least 3 h until just before inoculation, when the gas flow rate was adjusted as required. Due to the differing gas composition of all the gases tested, not all parameters could be kept constant simultaneously. The gas flow rate was adapted in each fermentation so that the total amount of carbon (the sum of CO_2 and CO) fed into the fermenter was approximately 0.4 mmol/min. As a result, the amount of H_2 fed to the fermenters differed between the experiments, at 0.2 mmol/min for the beech wood syngas (BWS) and 0.3 mmol/min for the lignin syngas (LS). For the fermentation of the BWS, the gas flow rate was controlled at 18 mL/min and for LS, the flow rate used was 23 mL/min.

Table 3 shows the average composition of the gas flow fed into the fermenter, measured after the reactor reached equilibrium, and under abiotic conditions, i.e. before inoculation. The gas flow fed into the fermenter equals then to that coming out in the off-gas.

Table 3. Gas composition and flow rates - values measured with process GC directly before inoculation

		H_2	CO	CO_2	CH_4	$CO+CO_2$	$H_2/(CO+CO_2)$	H_2/CO	Gas flow rate (NmL/min)
Beech wood	Composition (%)	27.0	21.3	18.0	10.6	39.3	0.7	1.27	23
	Molar flow (mmol/min)	0.28	0.22	0.19	0.10	0.41			
Lignin	Composition (%)	22.7	28.5	19.1	9.9	47.6	0.5	0.80	18
	Molar flow (mmol/min)	0.18	0.23	0.15	0.08	0.38			

Values are at Normal conditions at temperature of 0 °C (273.15 K) and absolute pressure of 1 atm (1.01325×105 Pa).

The fermenters' off-gas was analyzed using a GC-2010 Plus AT gas chromatograph (GC) (Shimadzu, Japan), with a ShinCarbon ST 80/100 Column (2 m × 0.53 mm ID, Restek, Germany) and a Rtx-1 capillary column (1 µm, 30 m × 0.25 mm ID, Restek, Germany). A thermal conductivity detector with helium as the carrier gas was used. The sampling regime was as follows: four samples of 2 mL were daily taken at 2 – 3 h intervals, with no sample collection taking place overnight. These were then used for OD (optical density) determination and left-over fructose and products (acetate and ethanol) concentration. The OD (optical density) was measured at 600nm, and OD and cell dry weight (CDW) correlation was determined as the average of 12 fermentations under comparable conditions (data not shown), with a resulting factor of CDW/OD = 0.3 g/L/OD. The sample collection, treatment, off-line analysis and data processing are described in detail elsewhere [8].

3. Results and Discussion

Gasification

Beech wood

In Figure 6, the temperature monitored by the four most important thermocouples placed within i-MILENA indirect gasifier, during gasification of beech wood, is shown. After the initial start-up, stable conditions were achieved for more than six hours, as indicated in the graph. The average temperature in the BFB gasification reactor, given by 3 thermocouples located at the bottom, middle and top part of the bed, during the steady operation, is around 860°C. The average temperature in the riser combustor is also 860°C. The small deviations in temperature at around 6.5 and 7.5 h are caused by a system disorder (instant pressure increase due to hampered hydrodynamics of the bed material).

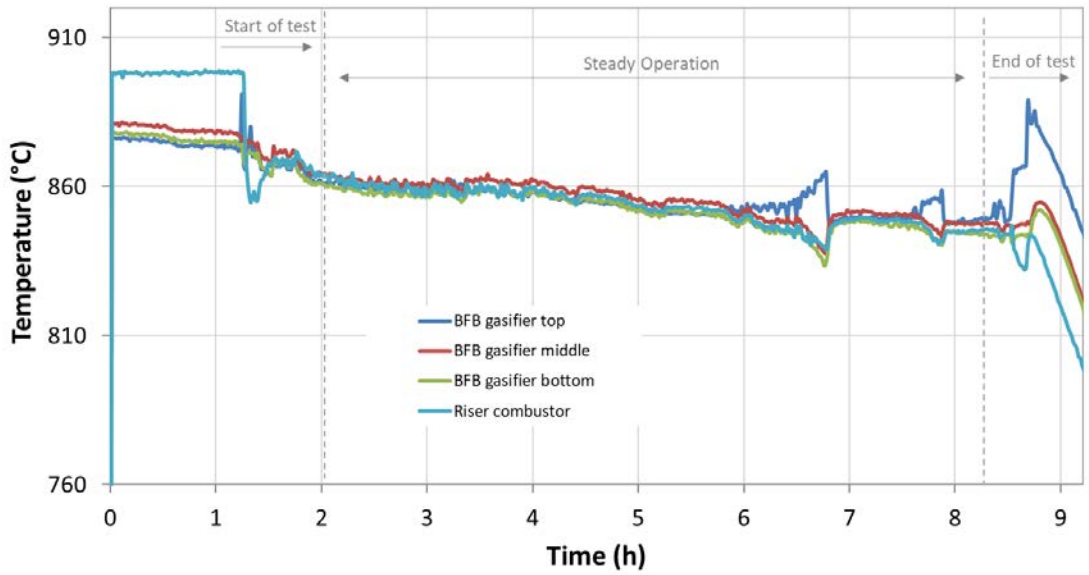

Figure 6. Temperature in the riser combustor and BFB gasifier bed zones of MILENA during beech wood gasification.

In Figure 7, the concentration of the main product gas components during the indirect gasification of beech wood, as measured at positions A and B, is presented. During the stable conditions the average composition of the gas – on dry basis – at position A (downstream MILENA) was 33.4 vol.% H_2, 28.0 vol.% CO, 23.8 vol.% CO_2 and 8.8 vol.% CH_4. However, 3.3 vol.% of the CO_2 is due to the CO_2 used as a carrier gas in the feeding screw and steam generator, as shown in Figure 2. The H_2/CO ratio was 1.2, which is a typical value for a woody biomass gasification test [28]. The use of olivine as bed material, results in enhanced H_2 production and decreased CO and CH_4 content compared to silica sand, due to its catalytic effect on the reforming of hydrocarbons and tar and the promotion of the water-gas shift (WGS) reaction [29, 30, 31]. At position B, downstream OLGA, H_2 and CO_2 concentration appear slightly reduced, while CO concentration is increased.

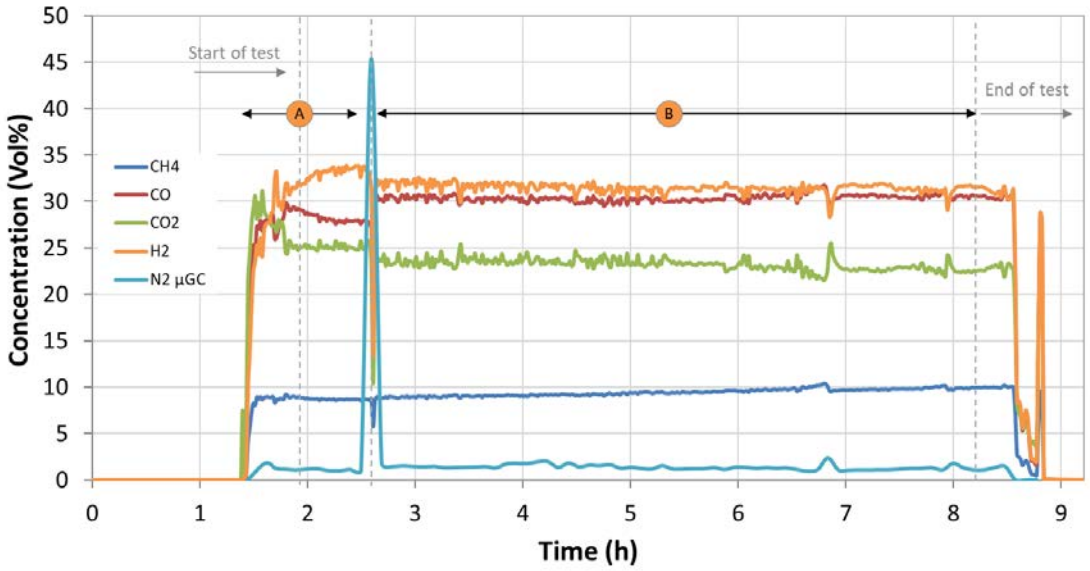

Figure 7. Concentration of the main gas components during beech wood gasification at positions A (downstream MILENA) and B (downstream OLGA), as measured by the online gas analyser.

The composition of the main gas components during beech wood gasification around the sampling positions C and E is shown in Figure 8 and reported in Table 4. During the stable conditions the average composition of the gas at position C (downstream the first AC bed) was identical to the gas measured at position B (downstream OLGA). The gas composition at position E (downstream HDS)

did not differ significantly to position C, the main difference was the H_2 concentration, which was lower at the outlet of the HDS reactor. This is because part of the inlet hydrogen in the gas is consumed by the hydrogenation on unsaturated C=C bonds and hydro-cracking reactions [32]. Additionally, methane concentration is slightly higher at the HDS outlet, due to the hydro-cracking reactions of the saturated hydrocarbons to methane [33, 34]. The main gas composition at position F (downstream the the ZnO and AC bed), before the bottling station, is shown in Figure 9 and Table 4 and it is similar to position E.

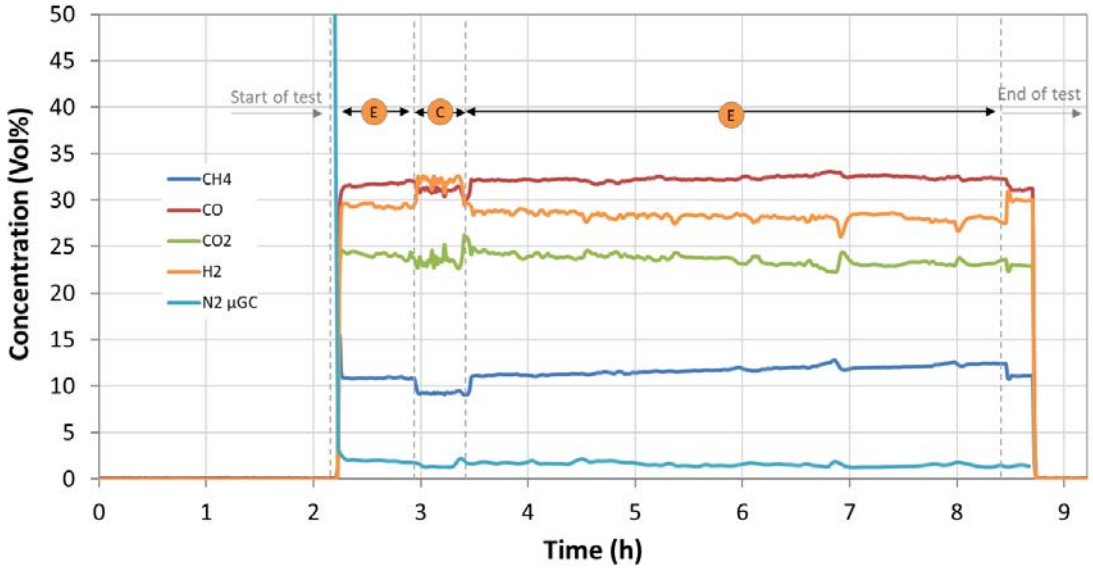

Figure 8. Concentration of the main gas components during beech wood gasification, at positions C (downstream the first AC bed) and E (downstream HDS), as measured by the online gas analyser.

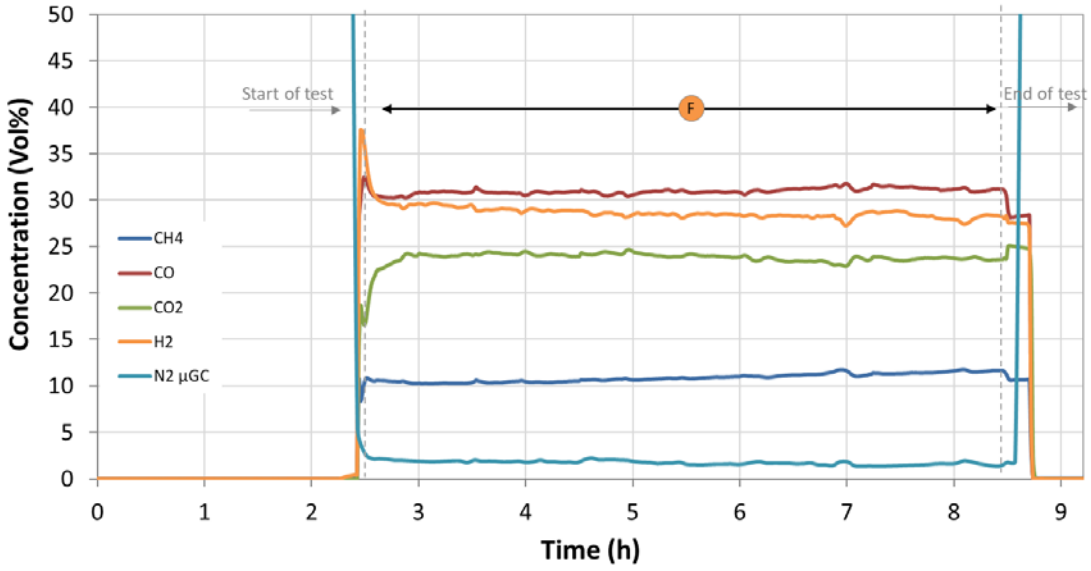

Figure 9. Concentration of the main gas components during beech wood gasification, at position F (downstream the ZnO and AC bed), as measured by the online gas analyser.

The composition of the trace sulphur and hydrocarbon compounds during beech wood gasification, at the sampling positions S1 and S2 is shown in Figure 10, Figure 11 and Table 4, as measured by the semi-online (every measurement takes approximately 4 min) µ-GC. The data points measured at position A (downstream MILENA) are limited and before the steady operation and therefore not very reliable. It is clear that the AC bed (position C) captures the bulk sulphur compounds (H_2S, COS). Downstream the HDS reactor (position E) the H_2S concentration increases slightly, due to the hydrodesulfurization of the mercaptans and the hydrolysis of carbonylsulfide, reactions that produce H_2S [32]. Benzene and toluene are captured by the BTX scrubber to below 100 and 10 ppmV, respectively. The unsaturated hydrocarbons, ethylene and acetylene, are hydrogenated in the HDS reactor to ethane [34] and therefore their concentration is reduced from 1.71 and 0.14 - respectively - to <0.001 vol%, with simultaneous increase of ethane concentration.

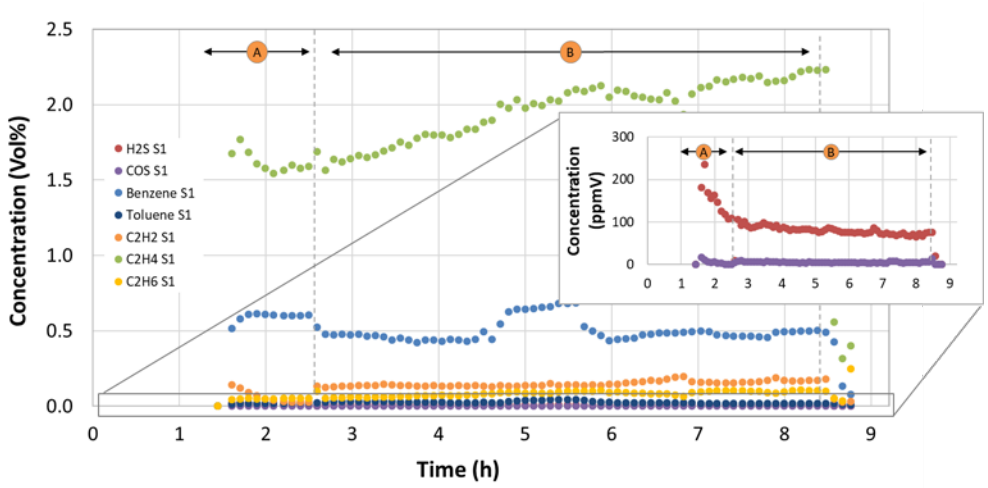

Figure 10. Concentration of the trace gas components during beech wood gasification at positions A (downstream MILENA) and B (downstream OLGA), as measured by the μ-GC.

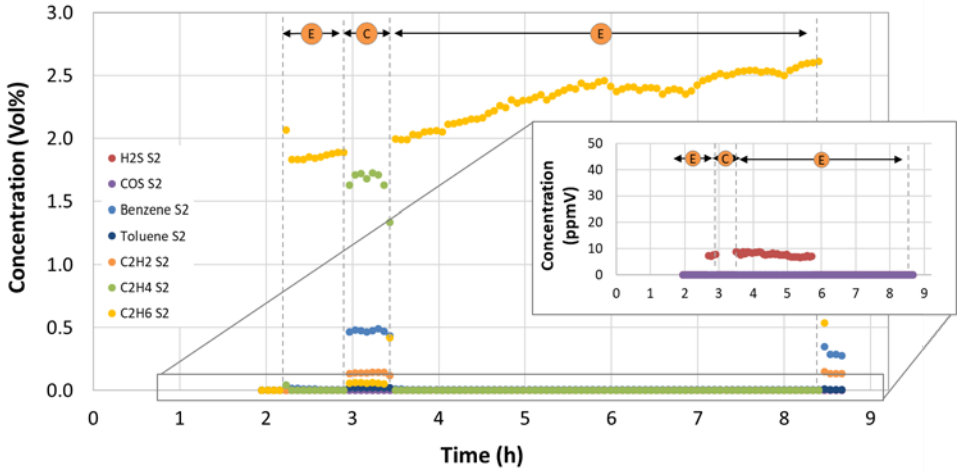

Figure 11. Concentration of the trace gas components during beech wood indirect gasification, at positions C (downstream the first AC bed) and E (downstream HDS), as measured by the μ-GC.

The concentration of the trace compounds at position F (downstream the ZnO and AC bed) is shown in Figure 12 and Table 4. All the undesired components are removed to below detection limit levels (10 ppmV) prior to gas bottling by the last AC and ZnO beds. Benzene concentration was <40 ppmV at the start of the bottling period but it was constantly reduced to around 10 ppmV by the end of the bottling procedure.

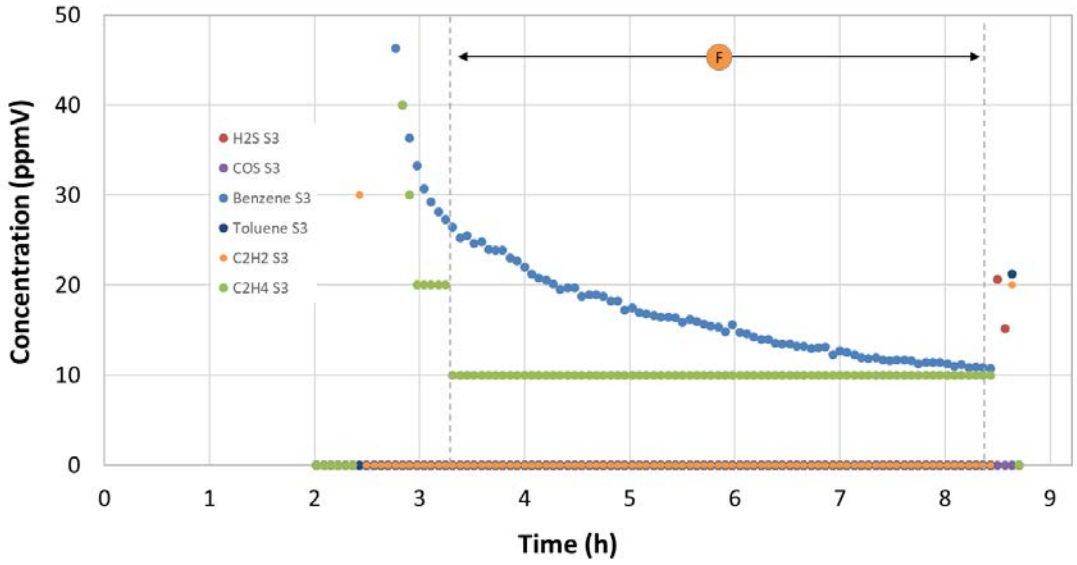

Figure 12. Concentration of the trace gas components during beech wood indirect gasification, at position F (after the ZnO and AC bed), as measured by the μ-GC.

In Table 4, the gas composition of the product gas, during indirect gasification of beech wood, is shown. The concentration of S-species (in the form of H_2S, COS and other S-organic components) was 120 ppmV in total. These low concentrations are attributed to the low content of the corresponding compounds, shown in Table 1.

The total tar concentration – on dry basis – in the raw product gas from beech wood gasification was 13 g/Nm^3. The main tar components formed were polyaromatic (2-ring) components, like naphthalene, along with small concentrations of other light and heavy polyaromatic hydrocarbons (e.g. acenaphtylene, phenanthrene). Aromatic (1-ring) components such as toluene, xylene and styrene, together with heterocyclic aromatic compounds, like cresol and phenol were also detected in smaller concentrations. Downstream OLGA, all tar compounds heavier than BTX were almost completely separated from the gas [7].

Table 4. Gas composition over the sampling positions S1, S2 and S3 during beech wood gasification and gas cleaning.

Gas component	Analysis method	Unit	Position A (Downstream MILENA)	Position B (Downstream OLGA)	Position C (Downstream AC)	Position E (Downstream BTX/HDS)	Position F (Downstream AC/ZnO)
Average sampling period (h)			**2 – 2.5**	**3 – 3.5**	**3 – 3.3**	**5 – 5.8**	**3 – 8**
CO	Gas monitor	Vol%	28.8	30.4	31.2	32.3	32.3
H_2	Gas monitor	Vol%	32.1	31.9	31.8	28.3	28.5

CO_2	Gas monitor	Vol%	25.2	21.9	22.4	23.2	23.3
CH_4	Gas monitor	Vol%	8.8	9.1	9.2	11.3	11.7
N_2	Gas monitor	Vol%	1.2	1.4	1.3	1.4	1.6
C_2H_2	micro GC	Vol%	0.03	0.14	0.14	<0.001	<0.001
C_2H_4	micro GC	Vol%	1.6	1.7	1.7	<0.001	<0.001
C_2H_6	micro GC	Vol%	0.05	0.06	0.06	2.37	2.49
Benzene	micro GC	ppmV	6022	4684	4746	86	13
Toluene	micro GC	ppmV	211	320	232	<10	<10
Sum C3	GC-FID	ppmV	85	113	103	291	323
Sum C4	GC-FID	ppmV	87	16	185	106	37
Sum C5	GC-FID	ppmV	51	1	83	17	63
Sum C6	GC-FID	ppmV	7	19	18	<1	8
H_2S	S-GC	ppmV	115	89	<0.5	7	<0.5
COS	S-GC	ppmV	4	6	0.8	<0.5	<0.5
Other S-	S-GC	ppmV	3	4	2	<0.5	<0.5
Ne tracer gas	micro GC	ppmV	-	898	935	932	964
Ar tracer gas	micro GC	Vol%	1.4	1.5	1.4	1.6	1.6
Tar content*	SPA	g/Nm^3	13.1	nd	nd	nd	nd

Values are at Normal conditions at temperature of 0 °C (273.15 K) and absolute pressure of 1 atm (1.01325×105 Pa).
nd: not determined
**Higher than toluene, on dry basis*

Lignin

In Figure 13, the temperature in i-MILENA indirect gasifier, during gasification of lignin, is shown. After the initial start-up, stable conditions were achieved for about 3 hours, as indicated in the graph. The average temperature in the combustor reactor - above the riser – was around 700°C, while the average temperature in the BFB gasifier, given by 3 thermocouples located at the bottom, middle and top part of the BFB, was 60°C higher, around 760°C. Higher temperature was expected in the riser combustor reactor than the BFB gasifier but since the lab-scale system was designed for normal MILENA operation, most of the heat input for gasification temperature control was provided from the external electric trace heating (at the outer part of the BFB reactor). This temperature difference between the gasifier and combustor reactor indicates that less char ends up in the combustor, which is attributed to poor circulation. After 4 hours on stream, the temperature in both the riser and the BFB reactor (especially at the bottom) is reduced. Due to the low gasification temperature, a cold zone located on top of the bed plate resulted in lower gas velocity than the critical point for fluidization and thus in

poor circulation of char and bed material. To compensate for reduced gas flow in the BFB, nitrogen was added occasionally for a couple of minutes (at 1, 3, 4.8 and 6 hours on stream), resulting in temperature increase (since more char was introduced in the riser combustor). Additionally, the lignin feeding rate was increased after 4.2 hours on steam to 3.5 kg/h but this was not sufficient as the temperature decreased again at around 5 hours on stream, therefore the steam rate was increased from 1 to 2.2 kg/h to compensate for reduced gas flow.

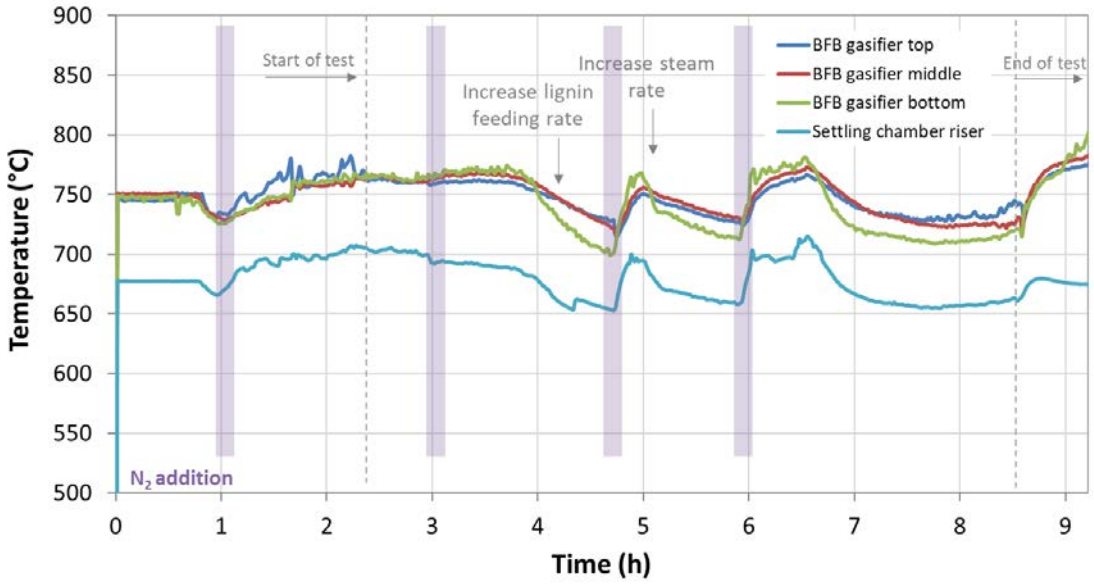

Figure 13. Temperature in the riser combustor and BFB gasifier bed zones of MILENA during lignin gasification.

The concentration of the main product gas components – on dry basis – during the indirect gasification of beech wood, as measured at positions A and B, is presented in Figure 14 and reported in Table 5. The values of H_2, CO_2 and CH_4 were similar to beech wood gasification but CO concentration appeared significantly lower, at 20 vol% compared to 30 vol% for beech wood. The effect of increased steam rate, after 5 hours on stream, was an increase in H_2 concentration that can be attributed to steam reforming and cracking reactions of the hydrocarbons [6]. In addition, the steam flow increase promotes the water gas shift reaction, resulting in higher H_2 and lower CO concentrations. The H_2/CO ratio is 1.8 which is much higher compared to beech wood gasification.

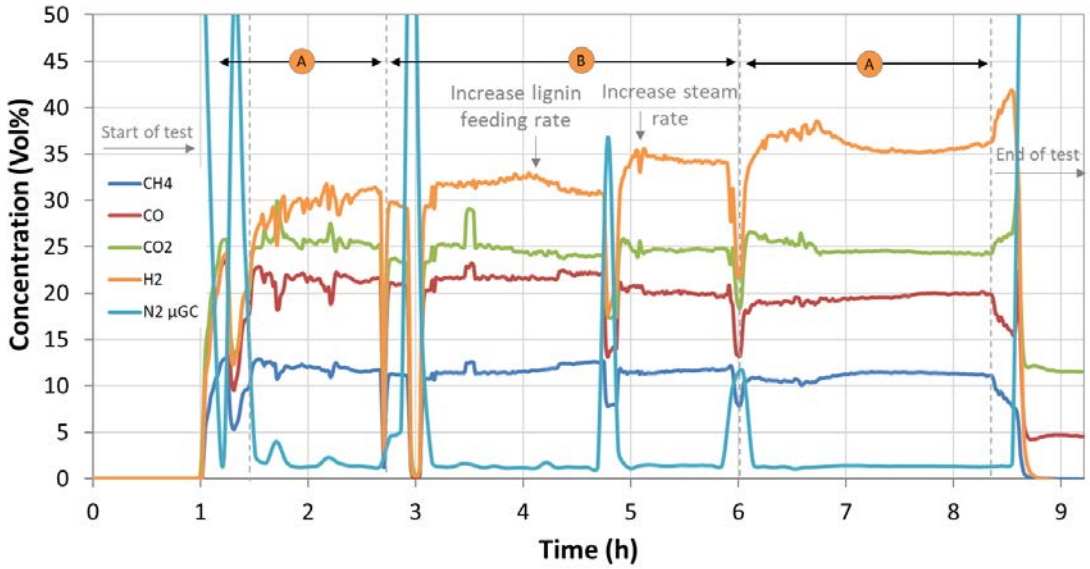

Figure 14. Concentration of the main gas components during lignin gasification at positions A (downstream MILENA) and B (downstream OLGA), as measured by the online gas analyser.

The composition of the main gas components during lignin gasification around the sampling positions C - E is shown in Figure 15 and reported in Table 5. The gas composition at position C (downstream AC bed) was identical to the gas measured at the MILENA/OLGA side. The composition at position E (downstream HDS) appeared more irregular due to N_2 evolution for the first hours on stream. This was attributed to the fact that the HDS reactor inlet valve was opened simultaneously with the gas analysis system at the outlet of the reactor and the HDS reactor was flushed overnight with N_2. This also affected the composition measured at position F (downstream ZnO and AC bed), shown in Figure 16, for the first 2 hours and resulted in slightly higher N_2 dilution in the first gas bottle. In general, lower H_2 concentration was observed at the HDS outlet compared to the inlet, similarly to the beech wood gasification. In addition, methane concentration was slightly higher at the HDS outlet, due to the hydro-cracking reactions between the saturated hydrocarbons and hydrogen. The main gas composition at position F (downstream ZnO and AC bed), before the bottling station, is shown in Figure 16 and Table 5 and it is similar to position E.

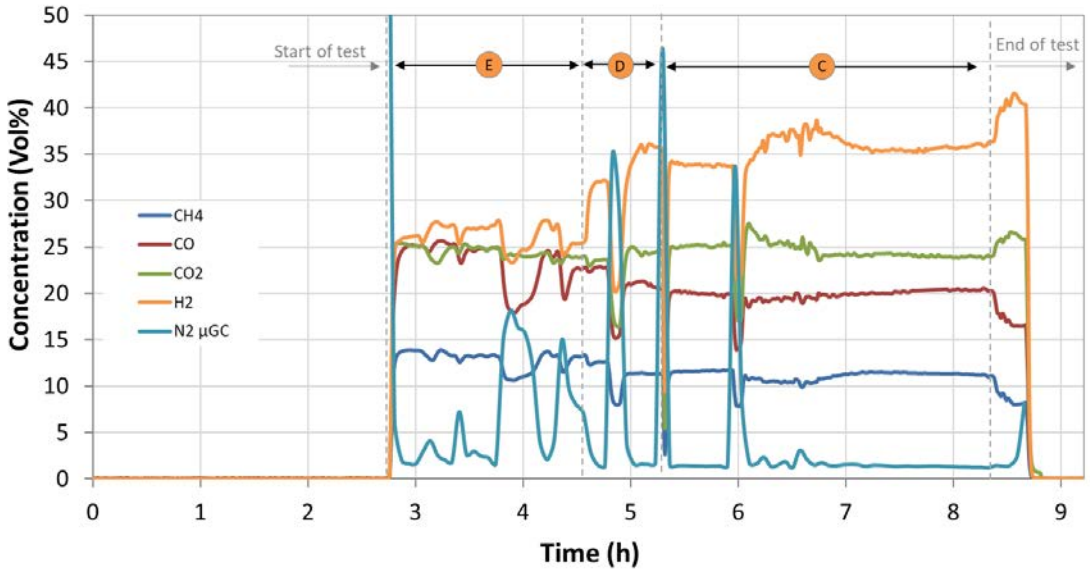

Figure 15. Concentration of the main gas components during beech wood gasification, at positions C (downstream the first AC bed), D (downstream BTX scrubber) and E (downstream HDS), as measured by the online gas analyser.

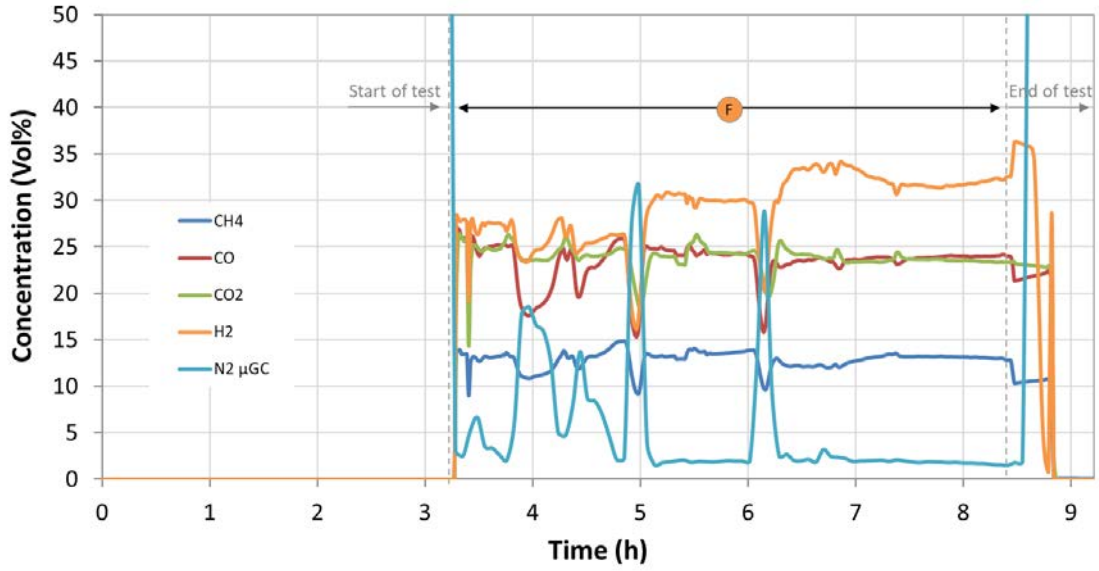

Figure 16. Concentration of the main gas components during beech wood gasification, at position F (downstream the ZnO and AC bed), as measured by the online gas analyser.

The composition of the trace sulphur and hydrocarbon compounds during lignin gasification, at the sampling positions S1 and S2 is shown in Figure 17, Figure 18 and Table 5. The concentration of Sulphur compounds in the gas (H_2S, COS) was around 10 times higher compared to beech wood gasification, which was expected due to the higher S-content in the original feedstock. C_{2+} hydrocarbons, including toluene, concentration was between 3 and 10 times higher than beech wood, which is attributed both to the lower gasification temperature that does not promote cracking reactions and to the the multi ring nature of the lignin molecule. The reduction of the C_2H_4 concentration with time on stream, measured at positions A and B, is due to the increase of steam rate that promotes cracking reactions of the hydrocarbons as mentioned earlier.

The AC bed (position C) captures the sulphur compounds, for instance H_2S concentration is reduced from 1000 ppmV (at position B) to 0.9 ppmV as measured by the GC-FPD (shown in Table 5), which is as low as the corresponding value in the beech wood test. Downstream the HDS reactor (position E) the H_2S concentration increases slightly to 10 ppmV, similar to the beech wood gasification test. Benzene and toluene are captured by the BTX scrubber to around 100 and 10 ppmV, respectively. The unsaturated hydrocarbons, ethylene and acetylene, are hydrogenated in the HDS reactor to ethane and their concentration is reduced from 3.5 and 0.62 - respectively - to <0.001 vol%, with simultaneous increase of ethane concentration.

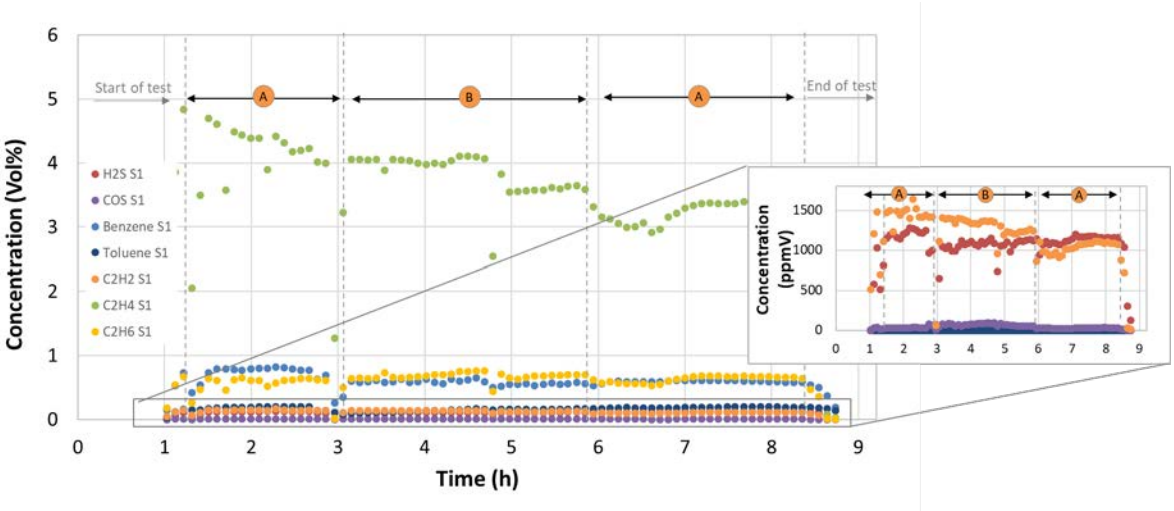

Figure 17. Concentration of the trace gas components during lignin gasification at positions A (downstream MILENA) and B (downstream OLGA), as measured by the μ-GC.

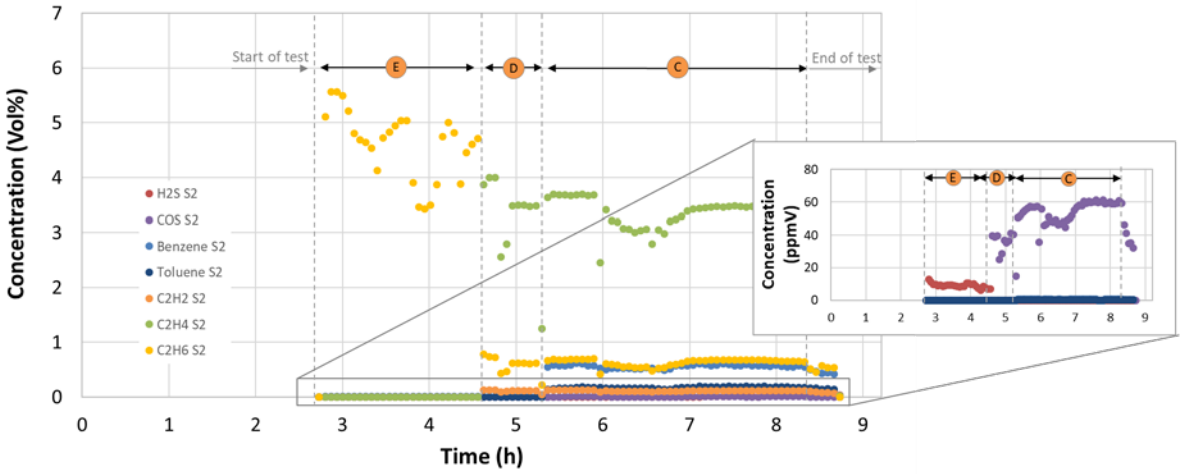

Figure 18. Concentration of the trace gas components during beech wood gasification, at positions C (downstream the first AC bed), D (downstream BTX scrubber) and E (downstream HDS), as measured by the μ-GC.

The concentration of the trace compounds at position F (downstream the ZnO and AC bed) is shown in Figure 19 and Table 5. All the undesired components are removed to below detection limit levels (10 ppmV) prior to gas bottling by the last AC and ZnO beds. Benzene concentration was <40 ppmV at the start of the bottling period but it was constantly reduced to around 10 ppmV by the end of the bottling procedure.

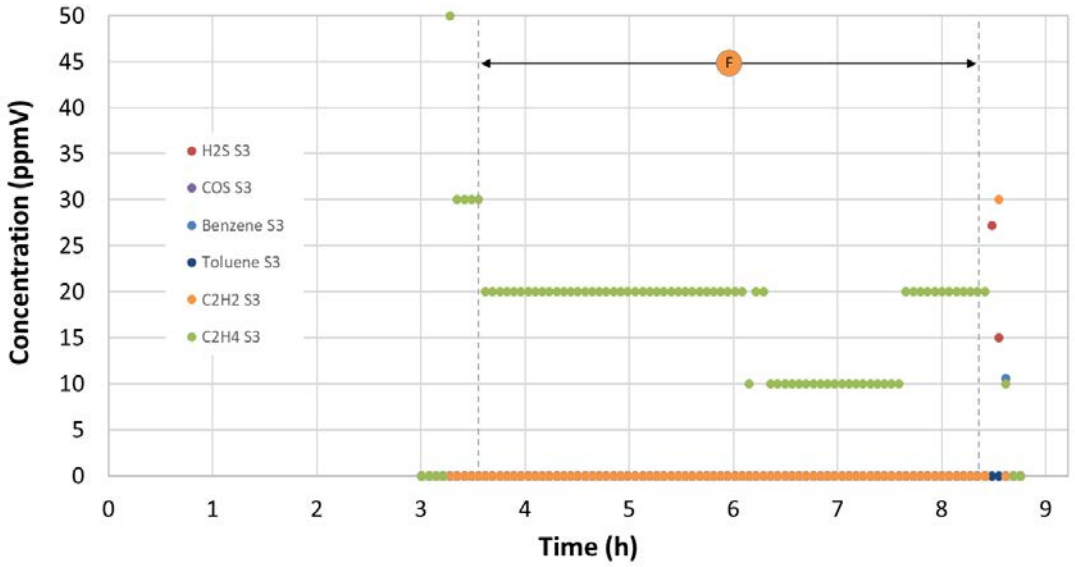

Figure 19. Concentration of the trace gas components during beech wood gasification, at position F (downstream the ZnO and AC bed), as measured by the μ-GC.

The total tar concentration – on dry basis – in the product gas from lignin gasification was 21 g/Nm^3, higher than of lignocellulosic biomass due to the multi ring nature of the lignin molecules which favours tar formation. The main tar components formed were polyaromatic (2-ring) components, like naphthalene, along with small concentrations of other light and heavy polyaromatic hydrocarbons (e.g. acenaphtylene, 2-methylnapthalene, phenanthrene). Heterocyclic aromatic compounds, like phenol, indene and cresol were also detected in significant concentrations. Aromatic (1-ring) components such as toluene, xylene and styrene, formed in small amounts. Again, all tar compounds heavier than BTX were almost completely separated from the gas downstream OLGA [7].

Table 5. Gas composition over the sampling positions S1, S2 and S3 during lignin gasification and gas cleaning.

Gas component	Analysis method	Unit	Position A (Downstream MILENA)	Position B (Downstream OLGA)	Position C (Downstream AC)	Position D (Downstream BTX)	Position E (Downstream HDS)	Position F (Downstream AC & ZnO)
Average sampling time (h)			**7 – 8.5**	**5.5 – 6**	**7 – 7.5**	**5 – 5.5**	**3 – 4.5**	**6.5 – 7**
CO	Gas monitor	Vol%	19.8	20.0	20.0	21.0	24.8	23.4
H_2	Gas monitor	Vol%	35.5	34.3	35.8	35.3	26.9	33.3

CO_2	Gas monitor	Vol%	24.4	24.7	24.2	24.5	24.8	24.1
CH_4	Gas monitor	Vol%	11.4	11.7	11.4	11.4	13.3	12.2
N_2	Gas monitor	Vol%	1.4	1.4	1.4	1.6	2.9	2.3
C_2H_2	micro GC	Vol%	0.11	0.12	0.12	0.12	<0.001	<0.001
C_2H_4	micro GC	Vol%	3.3	3.6	3.4	3.5	<0.001	<0.001
C_2H_6	micro GC	Vol%	0.67	0.69	0.67	0.62	4.47	4.43
Benzene	micro GC	ppmV	5972	5576	5897	109	122.5	<10
Toluene	micro GC	ppmV	1911	1609	1848	<10	12.4	<10
Sum C3	GC-FID	ppmV	3622	3113	4426	3290	3207	3380
Sum C4	GC-FID	ppmV	1494	1368	1830	1033	379	10
Sum C5	GC-FID	ppmV	809	736	851	171	31	<1
Sum C6	GC-FID	ppmV	<1	<1	<1	<1	<1	<1
H_2S	S-GC	ppmV	1165	1111	0.9[b]	0.2[c]	8.9	<0.5[e]
COS	S-GC	ppmV	31	55	50[b]	30[c]	0.7[d]	<0.5[e]
Other S-	S-GC	ppmV	50	33 [a]	42[b]	1[c]	<0.5[d]	<0.5[e]
Ne tracer gas	micro GC	ppmV	-	812	828	785	1121	768
Ar tracer gas	micro GC	Vol%	2.3	2.4	2.3	2.3	2.9	2.2
Tar content*	SPA	g/Nm^3	21.2	nd	nd	nd	nd	nd

Values are at Normal conditions at temperature of 0 °C (273.15 K) and absolute pressure of 1 atm (1.01325×105 Pa).
nd: not determined
**Higher than toluene, on dry basis*
[a] Gas bag sampled at 10:35, [b] Gas bag sampled at 12:50, [c] Gas bag sampled at 12:10, [d] Gas bag sampled at 11:25, [e] Gas bag sampled at 13:55

Syngas fermentation

Beech wood syngas

Substrate usage and carbon fixation

The fermentation was performed for a total of 93 h and the main fermentation products detected were acetate and ethanol, which is expected at these conditions [9] Table 6 shows the main fermentation results from the beech wood test: gas consumption profile, yields, productivity, acetate to ethanol ratio, as well as the percentage of carbon fixed. These parameters were calculated for the three different, relevant time frames: the complete run (endpoint), up to the point

when maximum CO consumption stopped (CO fixation) and during the interval of maximum overall usage. The percentage of carbon fixed ($E_{C, total}$), expressed in mol %, is the sum of CO_{used} and $CO_{2\ used}$ per total carbon fed (CO_{fed} plus CO_2, fed). If CO_2 is produced, then the sum of CO_{used} and CO_2, used is indeed CO_{fixed} [35]. Endpoint calculations were done using the values measured with the sample taken immediately before terminating the fermentation. A detailed explanation of the yield calculations (yield per substrate fed ($Y_{P/S, fed}$), yield per substrate used ($Y_{P/S, used}$), and yield per substrate fixed ($Y_{P/S, fixed}$)) and the terminology used can be found elsewhere [35].

Table 6. Main fermentation results, yield and productivity for the beech wood syngas

Interval		Unit	Endpoint	Closest to last point of maximum CO fixation	Maximum usage
Process time		h	93	38	17 – 38
$Y_{P/S, used}$		g/g	0.83	0.85	0.96
$Y_{P/S, fed}$		g/g	0.33	0.32	0.44
$Y_{P/S, fixed}$		g/g	0.97	0.94	1.02
$Y_{P/X}$		g/g	31.9	14.0	32
$V_{gas\ , fed}$		L	100.2	45.8	25.6
Acetate : Ethanol		mol/mol	7.8	16.3	14.5
Productivity	Acetate	g/L/h	0.17	0.17	0.26
	Ethanol	g/L/h	0.01	0.01	0.01
	Total	g/L/h	0.18	0.18	0.27
$E_{C,total}$		mol%	42.3	39.7	55.4

$Y_{P/S}$ = gram of products (acetate and ethanol) formed per gram of substrate (CO, CO_2 and H_2). This has been calculated per grams of substrate fed, used and fixed. $Y_{P/X}$ = gram of products (acetate and ethanol) per gram of cell dry weight. $P_{product}$ = productivity. Values are given as the average of a triplicate (n=3) with standard deviations. The error is ± 5-10%.

The amount of substance flow rate for H_2, CO and CO_2 detected in the bioreactor off-gas for the beech wood syngas fermentation with *C. ljungdahlii* is shown in Figure 20. The substrate usage and fixation for this fermentation is depicted in Figure 21.The peak observed in the off-gas graph (see Figure 20) and the sudden decreased in substrate usage or fixation (see Figure 21) between approximately 39 – 52 h of process time were due to an error on the set-up of the pH regulation that led to an increased fermenter volume of up to 1.7 L in all three bioreactors. At 43 h and 67 h of

process-time the excess fermentation broth was retrieved from the vessels bringing it down to the initial volume of 1.5 L. The amount of products and cell dry weight taken out from the fermenters have been taken into account in the calculations. Nonetheless, the pH was kept constant during this time. The smaller peaks at around 68 h seen in both Figure 20 and Figure 21 correspond to the addition of anti-foam to the fermenter, which causes a punctual alteration on the solubility of the gases in the fermenter broth.

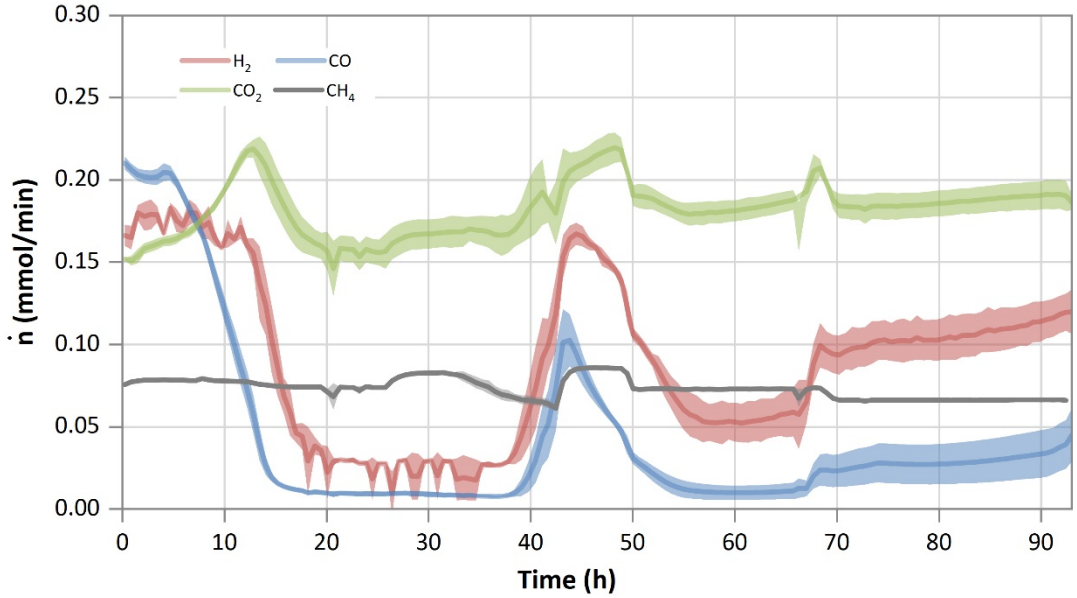

Figure 20. Amount of substance flow rate in the off-gas for beech wood syngas fermentation with C. ljungdahlii. Average measured amount of substance flow rate (ṅ) for hydrogen (red), carbon monoxide (blue), carbon dioxide (green) and methane (grey). Lines show the average of a triplicate (n=3), while the lighter coloured areas depict the standard deviation. A drop in the detected amount of substance in the off-gas compared to the initial starting value indicates the usage of that substance. The peaks observed between aprox. 40 and 55 h are the result of a pH malfunction.

During the first five hours of the fermentation, *C. ljungdahlii* mainly used up an average of 0.55 g/L of fructose carried over from the inoculation culture (data not shown). After that initial phase, the CO uptake rate increased constantly, as reflected by the decreasing amount of CO detected in the waste gas stream, up to the point when at 15 h of process-time the average detected amount of substance flow rate in the off-gas ($\dot{n}_{CO\ out}$) was below 0.02 mmol/min (Figure 1A). At 17 h, $\dot{n}_{CO\ out}$ had already decreased to 0.01 mmol/min, which corresponds to the point when the maximum CO fixation (> 85 %) started (Figure 2A). This continued for another 21 h, that is, up to 38 h after

inoculation, with an average CO fixation during this time of 91 %. Afterwards, due to the interference of the pH regulation issue, $\dot{n}_{CO\ out}$ increased until process-time 44 h, signaling a decrease in its usage. Nevertheless, it eventually increased again, reaching 70 % fixation at process-time 51 h, with an average of 79% until 64 h. After that, the fixation of CO started to decrease, being the average from this time up to the end of the process of 70%. From time 51 h to the end of the process, the average was 73%.

Looking at the CO usage (Figure 21), it stayed above 85% from 14 h to 40 h, with an average of 95%. The CO usage stayed below that threshold for 10 h, until process-time 50 h, due to the pH regulation glitch. Once it was fixed, it increased again above the 85% mark, staying so up to 90 h, with an average between those times of 91%. The value at 91 h was 84%, and it decreased to 80% at the end of the process (93 h).

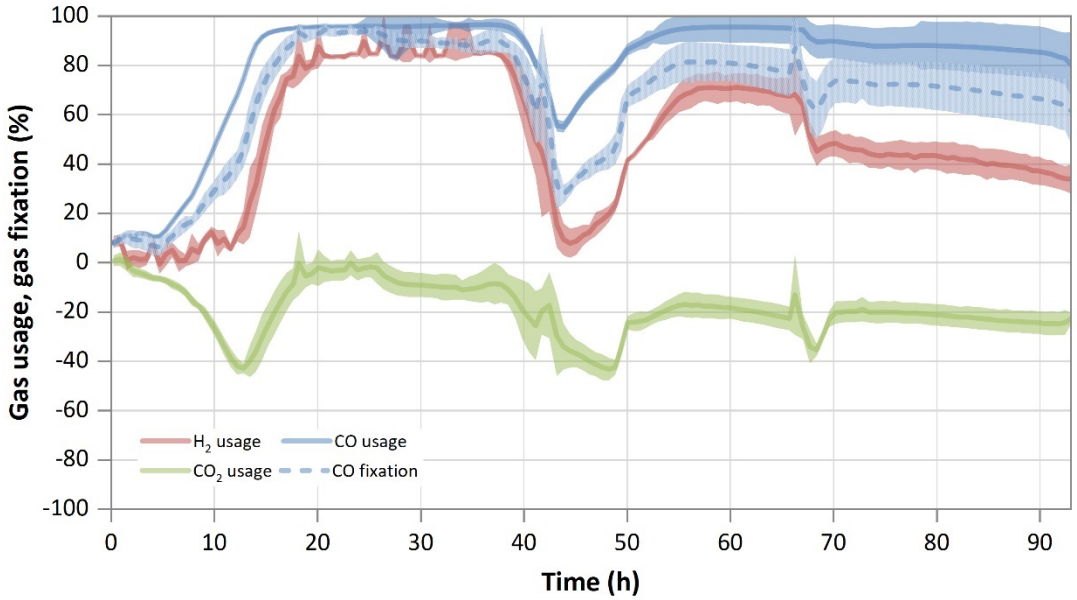

Figure 21. Substrate usage or fixation for beech wood syngas. Usage is shown for H_2 (red line), CO_2 (green line) and CO (blue line). CO fixation is depicted by the dotted blue line. The calculated difference between amount of substance flow rate fed into the bioreactor and the amount of substance flow rate detected in the off-gas is shown here as a percentage. For the CO fixation, if the CO_2 usage was negative, the amount of CO_2 produced was subtracted from the amount of (perceived) CO used. Lines show the average of a triplicate (n=3), while the lighter colored areas depict the standard deviation. The peaks observed between aprox. 40 and 55 h are the result of a pH malfunction.

Regarding H_2 uptake, a usage of ≥80 % was reached in average at 19 h after inoculation (Figure 21), when the off-gas analysis showed a detected gas flow rate of H_2 of 0.04 mmol/min (Figure 20). This persisted for at least 20 h, being the average usage during this interval 86% (Figure 21). Analogously to CO, the effect of the pH regulation malfunction can also be seen in the hydrogen off-gas analysis. The amount of H_2 detected increased rapidly from 38 h until 45 h of process-time, but after removing excess broth it decreased to a new minimum of 0.05 mmol/min at 61 h. The average between 45 h and 61 h for H_2 usage was 49 %. From this point on, and contrary to what is seen for CO, hydrogen usage did not recover its initial maximum values but rather decreased continuously until the end of the process, with an average in this case of 48%.

As shown in Figure 21, CO_2 was produced throughout the fermentation. The initial surge of CO_2 is due to the left-over fructose in the medium. As is the case for CO and H_2, the apparent increase in CO_2 production seen at process-time 43 h and 50 h was due to the malfunction of the pH regulation system. The maximum value measured for CO_2 outside that interval occurred at process-time 13 h, with a value of 0.22 mmol/min. Excluding the first 20 h (the initial peak was caused by fructose consumption), its usage value remained negative, indicating that there was a continuous CO_2 production, ranging from 0.05 % to 43 %.

The amount of CH_4 detected in the off-gas remained almost constant throughout the fermentation (shown in Figure 20). Before inoculation, an average of 0.08 mmol/min was measured, as shown in Table 3. The average maximum was around 0.09 mmol/min, and the average minimum, 0.06 mmol/min. The average for the whole run was 0.07 mmol/min. Again, the interference caused by the pH regulation fail can also be observed here between process-times 40 h and 50 h.

Finally, considering carbon fixation, the percentage of total carbon fixed per total carbon fed for the whole process was about 42%. For the interval up to 38 h, when maximum fixation of CO ceased, it reached 40% (Table 6).

Cell dry weight, product formation, yield and productivity

Figure 22 shows the cell dry weight growth and the products (acetate and ethanol) formation over time. During the first 20 hours, the CDW increased rapidly. Afterwards, growth slowed down and reached its maximum measured value of 0.62 g/L at 66.5 h. Following that, growth stopped and the CDW eventually decreased, with the last value recorded averaging at 0.57 g/L. With respect to product formation, acetate production starts immediately after inoculation, though the highest production rate was observed after 20 h. The final acetate concentration attained was 15.6 g/L. The ethanol concentration in the broth increased to 0.2 g/L at 19 h, reaching a value of 0.4 at 50 h of cultivation and finally attaining 1.6 g/L at the end of the process.

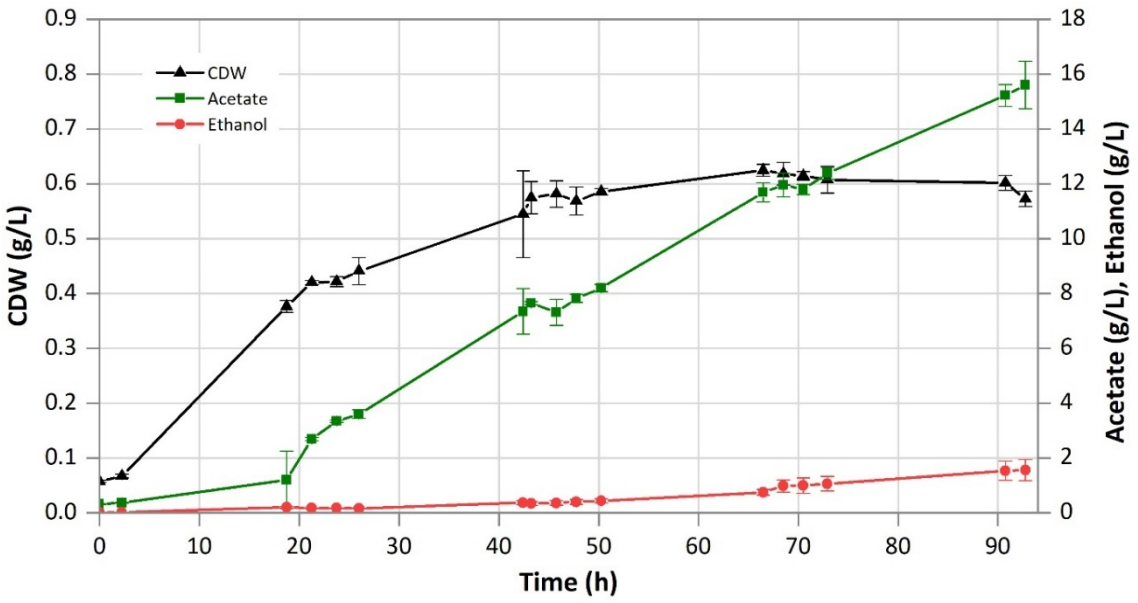

Figure 22. Growth and product formation profiles for beech wood syngas. Points indicate actual samples. Lines are only depicted for clarity purposes; error bars show the standard deviation among the triplicate. CDW = cell dry weight.

Product yields (acetic acid and ethanol) to total substrate fed ($Y_{P/S,\ fed}$), to used substrate ($Y_{P/S\ used}$), and to substrate fixed ($Y_{P/S\ fixed}$) are shown in Table 6 for each of the considered time spans: endpoint, up to the end of maximum CO fixation and during the interval of maximum overall usage. The highest $Y_{P/S}$ values were obtained during the maximum overall usage interval, with 0.44 (g/g of

total substrate fed), 0.96 (g/g of total substrate used) and 1.02 (g/g of substrate fixed). The highest acetate productivity (0.26 g/L/h) was also observed at this point, while ethanol productivity was 0.01 g/L/h for the three intervals. The acetate to ethanol molar ratio at the endpoint, was 7.8, as shown in Table 6.

Lignin syngas

Substrate usage and carbon fixation

The total process time for the lignin fermentation experiment was 93 h and the main products detected were acetate and ethanol, as in the beech wood test. Table 7 shows the main fermentation results from the lignin test: gas consumption profile, yields, productivity, acetate to ethanol ratio, as well as the percentage of carbon fixed, for the three different, relevant time frames.

Table 7. Main fermentation results, yield and productivity for the lignin syngas

Interval		**Unit**	**Endpoint**	**Closest to last point of maximum CO fixation**	**Maximum usage**
Process time		h	93	52	22 – 48
$Y_{P/S,\ used}$		g/g	0.79	0.89	0.84
$Y_{P/S,\ fed}$		g/g	0.30	0.32	0.40
$Y_{P/S,\ fixed}$		g/g	0.92	0.94	0.84
$Y_{P/X}$		g/g	31.8	18.9	33.4
$V_{gas\ ,\ fed}$		L	127.7	68.3	35.2
Acetate : Ethanol		mol/mol	5.2	17.4	16.2
Productivity	**Acetate**	g/L/h	0.16	0.19	0.23
	Ethanol	g/L/h	0.02	0.01	0.01
	Total	g/L/h	0.18	0.20	0.24
$E_{C,total}$		mol%	42.1	45.4	55.9

$Y_{P/S}$ = gram of products (acetate and ethanol) formed per gram of substrate (CO, CO_2 and H_2). This has been calculated per grams of substrate fed, used and fixed. $Y_{P/X}$ = gram of products (acetate and ethanol) per gram of cell dry weight. $P_{product}$ = productivity. Values are given as the average of a triplicate (n=3) with standard deviations. The error is ± 5-10%.

For the lignin fermentation, the amount of substance flow rate for H_2, CO and CO_2 detected in the bioreactor off-gas is shown in Figure 23, and the substrate usage and fixation for this fermentation are illustrated in Figure 24. In both Figure 23 and Figure 24, a small disturbance in the gas leaving the bioreactor can be seen around 45 h, which was caused by the addition of antifoam.

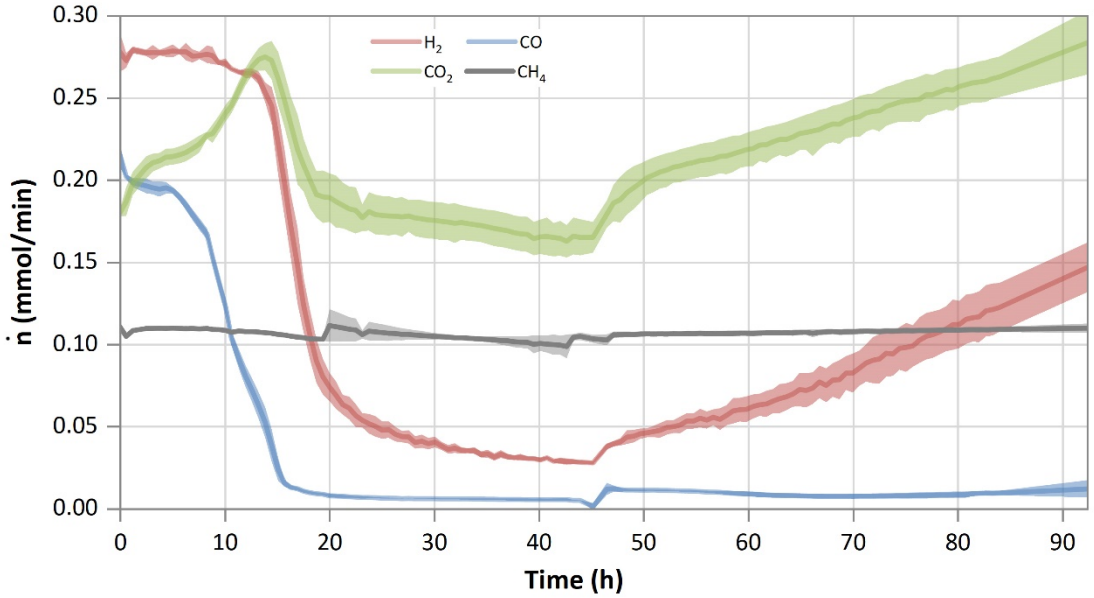

Figure 23. Amount of substance flow rate in the off-gas for lignin syngas. Average measured amount of substance flow rate (ṅ) for hydrogen (red), carbon monoxide (blue), carbon dioxide (green) and methane (grey). Lines show the average of a triplicate (n=3), while the lighter coloured areas depict the standard deviation. A drop in the detected amount of substance in the off-gas compared to the initial starting value indicates the usage of that substance.

As in the BWS fermentation, during the first 5 h approximately the microorganism used up an average of 0.54 g/L of fructose that were left as a carry-over from the inoculation culture (data not shown). CO uptake started directly afterwards (Figure 24), and $\dot{n}_{CO,out}$ at the off-gas decreased to below 0.02 mmol/min after 15.6 h of process-time (Figure 23). Both fermentations showed a comparable trend, with similar values for $\dot{n}_{CO,out}$ at similar times. Hence, it can be said that the different syngas source and composition did not have an impact on the performance of the cells during this first phase. At 18 h, $\dot{n}_{CO}$, out reached values below 0.01 mmol/min, corresponding to 87% fixation. This is the starting point for the maximum CO fixation interval, which continued for 34 h,

until process-time 52 h, as seen in Figure 24. The average CO fixation calculated for this time period is 95%. At 64 h of process-time, CO fixation was 77%, and the average between 52 h and 64 h was 81%. From 52 h of process-time up to the end of the fermentation the average for the percentage of carbon fixed was 73%. The average from 64 h to the end of the process was 68%.

It can be concluded that the microorganism performed consistently in both experiments, regarding CO fixation: firstly, the time that was required to reach 85 % CO fixation is equivalent in both cases: 17 h and 18 h for BWS and LS respectively. Despite not being able to compare the time period during which the pH glitch happened, after that, between 51 h (BWS) or 52 (LS) h and 64 h the average was 79 % and 81 % respectively. Finally, the behavior of *C. ljungdahlii* from 52 h to the end of the process was also almost identical in both cases.

CO usage reached 89% after 15 h and was maintained from that point throughout the duration of the process, at an average value of 96%, as opposed to what is seen with BWS, where a decrease is detected towards the end.

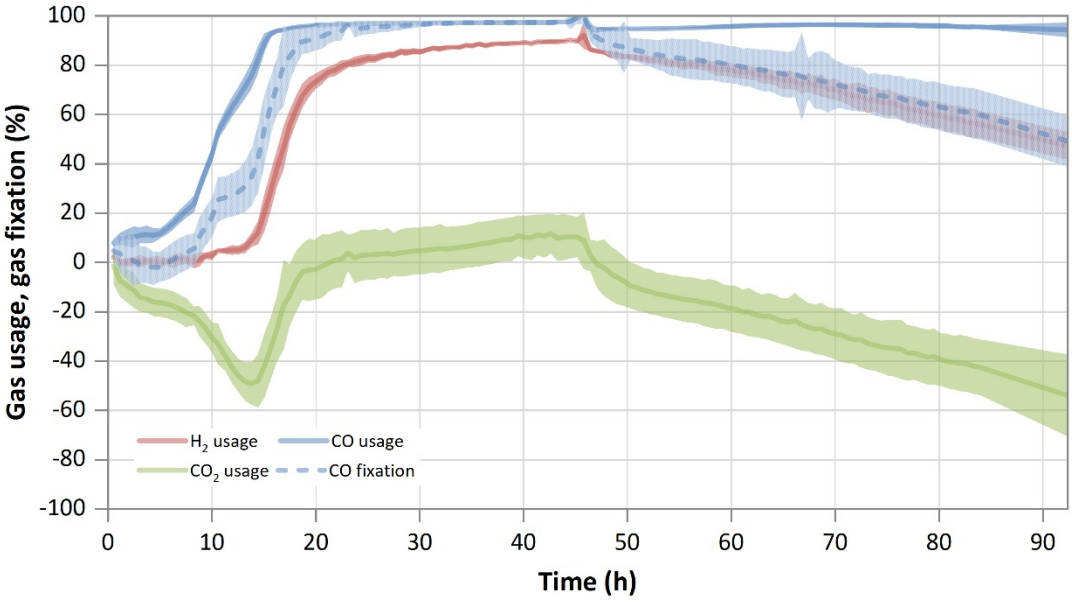

Figure 24. Substrate usage or fixation for lignin syngas. Usage is shown for H_2 (red line), CO_2 (green line) and CO (blue line). CO fixation is depicted by the dotted blue line. The calculated difference between amount of substance flow rate fed into the bioreactor and the amount of substance flow rate detected in the off-gas is shown here as a percentage. For the CO

fixation, if the CO_2 usage was negative, the amount of CO_2 produced was subtracted from the amount of (perceived) CO used. Lines show the average of a triplicate (n=3), while the lighter colored areas depict the standard deviation.

Concerning H_2, the threshold of 80% usage was achieved at 23 h and lasted for 34 h, until 57 h of process-time, as shown in Figure 24. From that point, where the flow detected in the off-gas was 0.06 mmol/min (see Figure 23), the amount of H_2 leaving the reactor steadily increased up to 0.15 mmol/min. The average usage between 57 h and the end sample was 68%, decreasing from 80% at the start of this interval to 47% at the end. Comparing the gas usage for both fermentations, it is observed that the graphs look similar (excluding the pH issue), having a first phase where H_2 is consumed at around 80 %, and then decreasing towards the end. It is interesting to notice that the flow rate of H_2 or the H_2:C_{total} ratio does not appear to have an effect on the gas usage, since even if it was lower in the BWS, with 0.18 mmol/min and 0.47, respectively, compared to 0.28 mmol/min and 0.69, respectively, in the LS, both fermentations performed similarly.

The initial increase in CO_2 production rate, as seen for the BWS fermentation, was due to the fermentation of the small amount of fructose left in the pre-culture. Even if the gas flow rate was adjusted so that the sum of CO_2 and CO was equivalent in both cases, and the CO_2 composition of both gases is similar (Table 3), CO_2 usage presented differences between BWS and LS. As opposed to what is seen in the BWS fermentation, where no CO_2 usage was seen at any time, in the LS fermentation CO_2 was used between process-time 22 h and 46 h (Figure 24), with an average of 6%. The maximum CO_2 usage achieved was 12% at 42.6 h, corresponding to a detected amount in the off-gas of 0.16 mmol/min (Figure 23). The variation in the range of values after 20 h was wider, compared to that of BWS: from 11.7% to -54%.

Finally, CH_4 remained stable, with a minimum and a maximum substance flow rate of 0.099 and 0.112 mmol/min, respectively, as shown in Figure 23. The average for the entire run was about 0.107 mmol/min. CH_4 did not appear to have any effect in the process, since the microorganisms lack

the ability to use it. It also did not produce any noticeable effect in growth or product formation, and can be considered, in this case, inert. This result is in line with what has been reported in the literature [36].

Regarding the other compounds present in both BWS and LS, such as C_2H_6, Ahmed et al. [12] showed that it also appears to not influence in any way the fermentation performance. C_2H_4 has been described as an inhibitor of methanogenic bacteria which inhibits the hydrogenases [37, 38]. At the concentration measured in the BWS (9 ppmV), and comparing the outcome with that of LS, which did not contain any C_2H_4 in measurable amounts, it can be said it did not cause any detrimental effect.

The percentage of total carbon that *C. ljungdahlii* was able to fix per carbon fed ($E_{C,total}$) during the entire LS fermentation (Table 7) was 42%, with 45% up to 52 h. . This parameter enables the comparison of the performance between different experiments, as well as serving as an indication of the fitness level of the cells at different stages of the fermentation. It is noticeable that not all carbon fed into the bioreactor could be captured, but in both cases, the calculated endpoint values are very similar. Therefore, it can be said that the different gas composition obtained from the gasification of beech wood and lignin did not influence the fermentation outcome in terms of affecting the ability of *C. ljungdahlii* to fix the carbon fed.

A previously reported fermentation, performed in the same system and under the same conditions but with a clean, commercially mixed syngas containing only CO, CO_2 and H_2 [35], has also been compared to the results obtained here. When the $E_{C,total}$ is considered, the clean syngas provided a higher carbon fixation ratio in all cases, achieving between 4 and 10% higher carbon fixation (data not published). This difference though cannot be solely attributed to the presence of impurities, since, as mentioned above, the gas composition was also different, and it is clear that this also has an impact in the fermentation outcome [36, 39].

Cell dry weight, product formation, yield and productivity

Figure 25 shows the cell dry weight growth and the products (acetate and ethanol) formation over time for the LS fermentation. The fastest increase in cell dry weight happened during the first 19 h of fermentation. Similar to the BWS fermentation, growth also slowed down afterwards, eventually coming to the non-growth phase (Table 3). The maximum CDW value was 0.61 g/L (at 66 h) before the growth stopped. At the process ending point, the value measured was 0.6 g/L (Figure 25). Both BWS and LS fermentations showed an almost identical profile regarding biomass production.

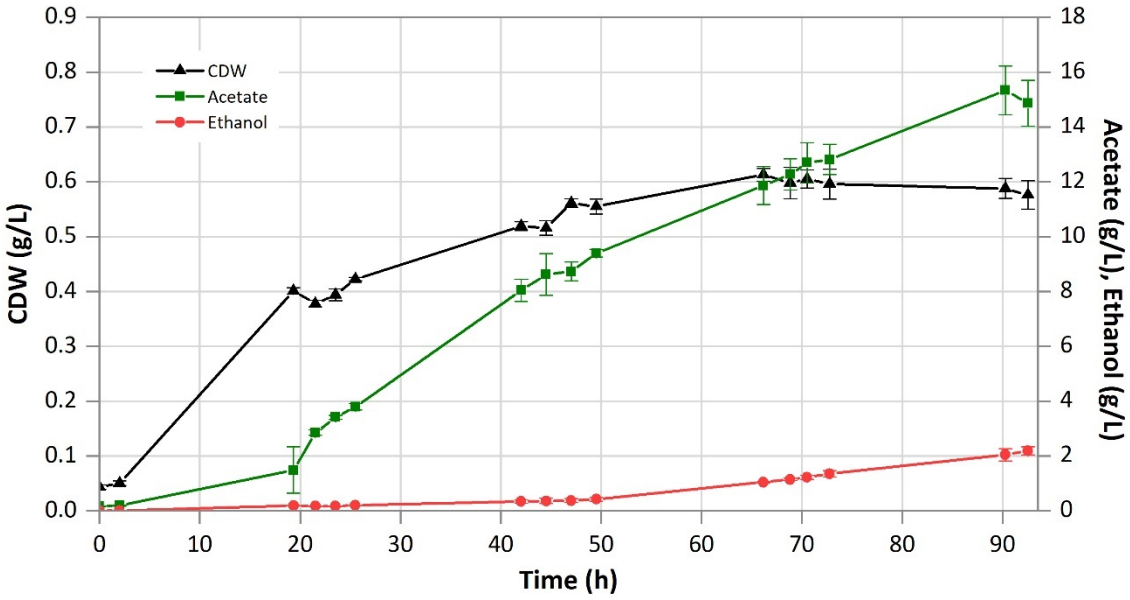

Figure 25. Growth and product formation profiles for lignin syngas. Points indicate actual samples. Lines are only depicted for clarity purposes; error bars show the standard deviation among the triplicate. CDW = cell dry weight.

Acetate formation could be detected already with the first samples, however the highest production rate was achieved after around 20 h, as in the beech wood syngas fermentation test. A slight decrease of the acetate production rate was observed after 45 h, with a final measured acetate concentration in the fermentation medium of 14.9 g/L, slightly lower than the BWS test. The ethanol concentration in the fermenter was 0.2 g/L after 19 h, and 0.4 after 50 h. The maximum reached at the end of the process amounted to 2.2 g/L, a bit higher than for BWS.

As shown in Table 7, also in this case the highest $Y_{P/S\ used}$ and $Y_{P/S\ fixed}$ obtained during the maximum overall usage period and was 0.40 and 0.84 g/g (of total fed substrate), respectively. Acetate productivity also reached its maximum during the same period: 0.23 g/L/h. Ethanol productivity was highest when calculated up to the end of the process: 0.02 g/L/h, while during the maximum usage and CO fixation intervals, it was 0.01 g/L/h. This is caused by the ethanol production starting towards the end of the process, after growth slows down, which is a well-documented behavior in *C. ljungdahlii* [40]. For the lignin syngas, the product profile at the endpoint was shifted towards ethanol, with a ratio of acetate to ethanol of 5.2. The other two intervals, on the contrary, presented a slightly higher ratio compared to beech wood.

End-point yields and productivities achieved are comparable for both BWS and LS. The most noticeable difference is found during the maximum usage interval, where BWS performed better than LS. Regarding product ratios, the LS fermentation presented a higher molar ethanol to acetate ratio at the endpoint, although it was the opposite at the other two intervals considered, suggesting that a metabolic shift happened towards the end of the fermentation.

Comparing the results with the fermentation of an impurity-free, synthetic-mixed syngas (32.5 % CO, 16.0 % CO_2 and 32.5 %H_2, with a flow rate of 18.0 L/min), with the same amount of total carbon (CO_2 + CO) fed (0.4 mmol C/min) [35], the product ratio was the same with the BWS (7.8 mol acetate/mol ethanol), while it was lower (5.2 mol acetate/mol ethanol) for LS (indicating, thus, more ethanol per acetate). Regarding productivities, at the endpoint it was 22% higher (0.22 g/L/h) than the BWS and LS fermentations (Table 6 and Table 7); up to the point of maximum CO fixation, it was 46% and 34% higher (0.27 g/L/h) than BWS and LS, respectively. During maximum overall usage the difference decreased, with the synthetic-mixed syngas being only 8% (0.26 g/L/h) above both BWS and LS. The yields achieved per substrate fed ($Y_{P/S,fed}$) at the endpoint by both the BWS and LS were also slightly lower: the synthetic-mixed syngas reached a value of 0.43 g/g, 23% and 30% higher than BWS and LS, respectively. Despite the negative impact of impurities in the syngas that has been

documented broadly in literature [13, 41, 42], the cleaning process applied in this case has been proven sufficient, as the endpoint yield per carbon fixed ($Y_{P/S, fixed}$) did not change significantly and remained mainly unaltered in the three cases.

4. Conclusions

This work demonstrated the combination of the lignin-rich residues gasification and gas cleaning with the syngas fermentation process, for the production of biofuels. Despite the different thermochemical properties of lignin compared to beech wood, the operational conditions applied during indirect gasification in i-MILENA resulted in a similar gas composition regarding the main gas components. Additionally, the gas cleaning steps applied downstream were able to reduce the impurities that could impose danger to the microorganism of the fermentation process, such as H_2S, COS, unsaturated hydrocarbons and aromatic compounds, resulting in similar gas qualities for both feedstocks. For comparison, in a study by Datar et al. [36], it was reported that the impurities present in the syngas after partial cleaning had a much greater impact. The fermentation of switch grass-generated syngas, caused both the inhibition of biomass growth and of H_2 usage of *Clostridium carboxidivorans P7*. The compounds present in the gas after the cleaning process applied were 4.2% CH_4, 2.4% C_2H_4 and 0.8% C_2H_6, as well as small concentrations of nitric oxide and acetylene.

The results presented here show the successful integration of biomass-generated syngas and fermentation, since no cell dormancy, or substrate consumption inhibition could be observed. The ethanol/acetate ratio remained constant for the beech wood syngas (BWS) and an increased ethanol production was observed for the lignin syngas (LS). Therefore, the product gas cleaning process applied for both beech wood and lignin feedstocks, is sufficient for using the gas as fermentation substrate by *C. ljungdahlii*. Nonetheless, further optimization studies will be needed to achieve a better carbon fixation capacity, as well as to boost productivities, to improve the economic feasibility of the overall process.

Not many studies have used biomass-derived syngas as fermentation substrate, and even fewer report the linking of the gasification and fermentation technology. In two other instances described in literature, the impurities present in the syngas have been reported to have a much greater impact. Here, it could be shown that both BWS and LS caused no significant detrimental effects on the cultures. This is a crucial point, since biomass-derived syngas is reported to have caused the microorganisms to cease growing, as well as negatively impact H_2 consumption, which stopped after the biomass-derived gas was introduced [12, 36]. It must be noted, though, that the syngas generated in those studies had a much lower H_2 content and lower CO_2 concentration [36].

Moreover, in a calculation based on the commercial LanzaTech process [10], the carbon conversion efficiency results in 51.6 %. In this study, values around 55 % for carbon fixation onto products are achieved for both BWS and LS during maximum usage interval, showing that this system has potential to be further developed. 99 % of the carbon fixed could be detected in the products and biomass, with the remaining used carbon being accounted for as produced CO_2. The performance of this process is comparable to the one reported in literature [12], where 97 % of the utilized carbon could be detected in biomass and product as well as CO_2 formation.

Compared to the synthetic-mixed syngas, where no other unidentified trace compounds were present, no difference in the ethanol/acetate ratio was observed for the BWS, but an increased ethanol production could be seen towards the end in LS, similar to other studies [12, 36]. The reason why ethanol production did not increase in BWS compared synthetic-mixed syngas remains to be investigated. A potential reason could be the difference in the gas composition, known to affect the fermentation outcome [16]. Most studies found in literature are focused on the effects of the ratio of only two of the syngas components (CO/CO_2, H_2/CO_2, CO/H_2), without any impurity present. The combined synergistic effects of different $CO/CO_2/H_2$ blends, together with impurities, has not been widely considered. Valgepea et al. found that more ethanol was produced by *Clostridium autoethanogenum* when grown on H_2/CO compared to when grown on pure CO, but in the case here

presented, the higher H_2/CO ratio of the BWS did not cause this effect [43]. This highlights the need for more research efforts towards linking the gasification and fermentation technologies, and the limitation of extrapolating results from clean gas mixtures to biomass-derived syngas. Hurst and Lewis [44] reported that, when growing *Clostridium carboxidivorans P7* in CO/CO_2 gas mixtures, an increase of the CO partial pressure resulted in increased ethanol production. Higher CO concentrations also directed *Clostridium ljungdahlii* product formation towards ethanol when grown with H_2/CO [45]. Hence, the higher amount of CO present in the LS could be a reason for the higher ethanol production, compared to BWS.

As a next step, the effect of some impurities, such as the unsaturated hydrocarbons and the S-compounds, should be studied on the fermentation process by *Clostridium ljungdahlii*. This would result in a simpler gas cleaning process, thus reducing the cost. Additionally, the fermentation of biomass-derived syngas in a continuous process would be of use in order to assess productivities and yields over a longer term, where cells are exposed to impurities during a prolonged period of time.

Acknowledgements

This work has received finding from the European Union's Horizon 2020 research and innovation programme under grant agreement No. 731263.

References

[1] Ambition research official website: https://www.ambition-research.eu/ [Accessed on 10-2-2020].
[2] M.P. Pandey, C.S. Kim, Lignin depolymerization and conversion: a review of thermochemical methods, Chem. Eng. Technol. 34 (2011) 29–41.
[3] N. Cerone, F. Zimbardi, L. Contuzzi, M. Prestipino, M.O. Carnevale, Air-steam and oxy-steam gasification of hydrolytic residues from biorefinery. Fuel Process. Technol. 167 (2017) 451-461. doi: 10.1016/j.fuproc.2017.07.027
[4] N. Cerone, F. Zimbardi, L. Contuzzi, E. Alvino, M.O. Carnevale, V. Valerio, Updraft gasification at pilot scale of hydrolytic lignin residue, Energy Fuel 28 (2014) 3948–3956.

[5] F. Pinto, R.N. Andre, C. Carolino, M. Miranda, P. Abelha, D. Direito, J. Dohrup, H.R. Sorensen, F. Girio, Fuel 140 (2015) 62-72.
[6] E.T. Liakakou, B.J. Vreugdenhil, N. Cerone, F.Zimbardi, F. Pinto, R. André, P. Marques, et al. Fuel 251 (2019) 580-592. https://doi.org/10.1016/j.fuel.2019.04.081
[7] Yen-Ting Kuo, G. Aranda Almansa, B.J. Vreugdenhil, Catalytic aromatization of ethylene in syngas from biomass to enhance economic sustainability of gas production, Applied Energy 215 (2018) 21-30. https://doi.org/10.1016/j.apenergy.2018.01.082
[8] F. Oswald, S. Dörsam, N. Veith, M. Zwick, A. Neumann, K. Ochsenreither, C. Syldatk, Sequential Mixed Cultures: From Syngas to Malic Acid. Front. Microbiol. 7:891 (2016) 1-12. doi: 10.3389/fmicb.2016.00891
[9] F.M. Liew, M.E. Martin, R.C. Tappel, B.D. Heijstra, C. Mihalcea, M. Köpke (2016) Gas Fermentation – A Flexible Platform for Commercial Scale Production of Low Carbon Fuels and Chemicals from Waste and Renewable Feedstocks. Front. Microbiol. 7:694, 1–28. doi:10.3389/fmicb.2016.00694.
[10] D.W. Griffin, M.A. Schultz (2012). Fuel and Chemical Products from Biomass Syngas: A Comparison of Gas Fermentation to Thermochemical Conversion Routes. Environ. Prog. Sustain. Energy 31, 219–224. doi:10.1002/ep.
[11] J. Daniell, M. Köpke, M., S.D. Simpson (2012). Commercial Biomass Syngas Fermentation. Energies 5, 5372–5417. doi:10.3390/en5125372.
[12] A. Ahmed, B.G. Cateni, R.L. Huhnke, R.S. Lewis, (2006). Effects of biomass-generated producer gas constituents on cell growth, product distribution and hydrogenase activity of *Clostridium carboxidivorans* P7T. Biomass and Bioenergy 30, 665–672. doi:10.1016/j.biombioe.2006.01.007.
[13] D. Xu, D.R. Tree, R.S. Lewis (2011). The effects of syngas impurities on syngas fermentation to liquid fuels. Biomass and Bioenergy 35, 2690–2696. doi:10.1016/j.biombioe.2011.03.005.
[14] K.D. Ramachandriya, D.K. Kundiyana, A.M. Sharma, A. Kumar, H.K. Atiyeh, R.L. Huhnke, M.R. Wilkins, Critical factors affecting the integration of biomass gasification and syngas fermentation technology, AIMS Bioengineering, 3 (2016) 188-210. doi: 10.3934/bioeng.2016.2.188.
[15] 09/08, N. p. (2009). Review of Technologies for Gasification of Biomass and Wastes,UK: E4tech, NNFCC.
[16] K.M. Hurst, R.S. Lewis, Carbon monoxide partial pressure effects on the metabolic process of syngas fermentation. Biochem. Eng. J. 48 (2010) 159–165.
[17] K. Liu, H.K. Atiyeh, R.S. Tanner M.R. Wilkins, R.L. Huhnke, Fermentative production of ethanol from syngas using novel moderately alkaliphilic strains of *Alkalibaculum bacchi*. Bioresour. Technol. 102 (2012) 336–341. doi: 10.1016/j.biortech.2011.10.054
[18] K. Chandolias, T. Richards, and M. J. Taherzadeh (2018) Combined gasification-fermentation process in waste biorefinery, in Waste Biorefinery : Potential and Perspectives, 157-200. Elsevier Ltd. https://doi.org/10.1016/B978-0-444-63992-9.00005-7
[19] J. Mock, Y. Zheng, A.P. Mueller, S. Ly, L. Tran, S. Segovia, et al. Energy conservation associated with ethanol formation from H_2 and CO_2 in *Clostridium autoethanogenum* involving electron bifurcation. J Bacteriol. 2015;197:2965–80. doi: 10.1128/JB.00399-15
[20]A. Kumar, K. Eskridge K, D.D. Jones, M.A. Hanna (2009) Steam–air fluidized bed gasification of distillers grains: Effects of steam to biomass ratio, equivalence ratio and gasification temperature. Bioresource Technol 100: 2062–2068. DOI: 10.1016/j.biortech.2008.10.011
[21] B.D. Heijstra, C. Leang, A. Juminaga, Gas fermentation: cellular engineering possibilities and scale up, Microb Cell Fact 16, 60 (2017). https://doi.org/10.1186/s12934-017-0676-y
[22] Teixeira LV, Moutinho LF, Romao-Dumaresq AS. Gas fermentation of C1 feedstocks: commercialization status and future prospects. Biofuels Bioprod Bioref 2018;12:1103–17. https://doi.org/10.1002/bbb.1912.
[23] Lane J. On the mend: Why INEOS Bio isn't producing ethanol in Florida. Biofuels Dig. 2014. http://www.biofuelsdigest.com/bdigest/2014/09/05/on-the-mend-why-ineos-bio-isnt-reporting-much-ethanol-production/ [Accessed on 13-5-20]
[24] B. Karlson, C. Bellavitis, N. France, J. Manage. Organ. 2018, 1–22. DOI: https://doi.org/10.1017/jmo.2017.83
[25] Sekisui chemical co., ltd. Turning "Garbage" into Ethanol: https://www.sekisuichemical.com/whatsnew/2017/1325318_29675.html [Accessed on 20-5-2020]
[26] E.R. Widjaya, G. Chen, L. Bowtell, C. Hills. Gasification of non-woody biomass: a literature review. Renew Sustain Energy Rev 2018;89:184–93. https://doi.org/10.1016/j.rser.2018.03.023.
[27] L. E. Fryda, K. D. Panopoulos, E. Kakaras, Powder Technology 181, 3 (2008) 307-320. https://doi.org/10.1016/j.powtec.2007.05.022
[28] C.M. van der Meijden (2010). Development of the MILENA gasification technology for the production of BioSNG, Eindhoven: Technische Universiteit Eindhoven DOI: 10.6100/IR691187.

[29] M. Virginie, J. Adanez, C. Courson, L.F. de Diego, Effect of Fe-olivine on the tar content during biomass gasification in a dual fluidized bed, Applied Catalysis B: Environmental, 121–122 (2012) 214–222.
[30] L. Devi (2005). Catalytic removal of biomass tars, Olivine as prospective in-bed catalyst for fluidized-bed biomass gasifiers, Doctoral Thesis, Eindhoven University of Technology, ISBN: 90-386-2906-0.
[31] G. Aranda, A. van der Drift, B.J. Vreugdenhil, H.J.M. Visser, C.F. Vilela, C.M. van der Meijden Comparing direct and indirect fluidized bed gasification: effect of redox cycle on olivine activity, Environ. Prog. Sustainable Energy, 33 (2014), 711-720.
[32] R.A. Sánchez-Delgado (2007) Hydrodesulfurization and Hydrodenitrogenation, in D. Michael P. Mingos and R.H. Crabtree (Eds), Comprehensive Organometallic Chemistry III, From Fundamentals to Applications, 759-800. Elsevier Ltd. DOI: 10.1016/B0-08-045047-4/00029-7
[33] J. Horáček, D. Kubička, Bio-oil hydrotreating over conventional CoMo & NiMo catalysts: The role of reaction conditions and additives, Fuel 198 (2017) 49-57. https://doi.org/10.1016/j.fuel.2016.10.003.
[34] H. Wang, G. Li, K. Rogers, H. Lin, Y. Zheng, S. Ng, Hydrotreating of waste cooking oil over supported CoMoS catalyst – Catalyst deactivation mechanism study, Molecular Catalysis 443 (2017) 228-240
[35] A. Infantes, M. Kugel, A. Neumann (2020). Evaluation of Media Components and Process Parameters in a Sensitive and Robust Fed-Batch Syngas Fermentation System with *Clostridium ljungdahlii*. Fermentation. doi: 10.3390/fermentation6020061
[36] R.P. Datar, R.M. Shenkman, B.G. Cateni, R.L. Huhnke, R.S. Lewis (2004). Fermentation of biomass-generated producer gas to ethanol. Biotechnol. Bioeng. 86, 587–594. doi:10.1002/bit.20071.
[37] G.D. Sprott, K.F. Jarrell, K.M. Shaw, R. Knowles (1982). Acetylene as an inhibitor of methanogenic bacteria. J. Gen. Microbiol. 128, 2453–2462. doi:10.1099/00221287-128-10-2453.
[38] N.A. Zorin, B. Dimon, J. Gagnon, J. Gaillard, P. Carrier, P.M. Vignais (1996). Inhibition by iodoacetamide and acetylene of the H-D-exchange reaction catalyzed by *Thiocapsa roseopersicina* hydrogenase. Eur. J. Biochem. 241, 675–681. doi:10.1111/j.1432-1033.1996.00675.x.
[39] F.R. Bengelsdorf, M. Straub, P. Dürre (2013). Bacterial synthesis gas (syngas) fermentation. Environ. Technol. 34, 1639–1651. doi:10.1080/09593330.2013.827747.
[40] H. Richter, B. Molitor, H. Wei, W. Chen, L. Aristilde, L.T. Angenent (2016). Ethanol production in syngas-fermenting *Clostridium ljungdahlii* is controlled by thermodynamics rather than by enzyme expression, Energy Environ. Sci. 9, 2392-2399. doi: 10.1039/C6EE01108J
[41] P.C. Munasinghe, S.K. Khanal (2011). Biomass-derived syngas fermentation into biofuels: Opportunities and challenges. Biofuels 101, 79–98. doi:10.1016/B978-0-12-385099-7.00004-8.
[42] K.D. Ramachandriya, D.K. Kundiyana, A.M. Sharma, A. Kumar, H.K. Atiyeh, R.L. Huhnke, et al. (2016). Critical factors affecting the integration of biomass gasification and syngas fermentation technology. AIMS Bioeng. 3, 188–210. doi:10.3934/bioeng.2016.2.188.
[43] K. Valgepea, R.S.P. Lemgruber, T. Abdalla, S. Binos, N. Takemori, A. Takemori, et al. (2018). H_2 drives metabolic rearrangements in gas-fermenting *Clostridium autoethanogenum*. Biotechnol Biofuels 11:55. doi: 10.1186/s13068-018-1052-9
[44] K.M. Hurst, R.S. Lewis (2010). Carbon monoxide partial pressure effects on the metabolic process of syngas fermentation. Biochem. Eng. J. 48;2, 159-165. doi: 10.1016/j.bej.2009.09.004
[45] J. Jack, J. Lo, P-C. Maness, Z.J. Ren (2019). Directing *Clostridium ljungdahlii* fermentation products via hydrogen to carbon monoxide ratio in syngas. Biomass and Bioenergy 124, 95-101. doi: 10.1016/j.biombioe.2019.03.011